IMPROVEMENT OF MOBILE TRILATERATION ACCURACY WITH MODIFIED GEO-LOCATION TECHNIQUES

Thesis submitted for the fulfillment of requirements for the degree of

MASTER OF SCIENCE

in

Electronic Engineering

By

Robson Takudzwa Reza

COLLEGE OF AGRICULTURE, ENGINEERING AND SCIENCE
UNIVERSITY OF KWAZULU-NATAL, DURBAN - 4041
SOUTH AFRICA

STUDENT NO.: 217079153

MARCH 2018

IMPROVEMENT OF MOBILE TRILATERATION ACCURACY WITH MODIFIED GEO-LOCATION TECHNIQUES

Student:

Robson Takudzwa Reza

Supervisor:

Prof. (Dr.) Viranjay M. Srivastava

This thesis submitted in fulfilment of the requirements for the degree of

Master of Science (Electronic Engineering)

At

Howard College, School of Engineering,

University of KwaZulu-Natal, Durban – 4041,

South Africa.

As the candidate’s supervisor, I have approved this thesis for submission.

Signed…….. .. Date……..

Name: Prof. (Dr.) Viranjay M. Srivastava

DECLARATION 1

PLAGIARISM

I, **Robson Takudzwa Reza** with student number 217079153, declare this thesis titled ***"IMPROVEMENT OF MOBILE TRILATERATION ACCURACY WITH MODIFIED GEO-LOCATION TECHNIQUES"*** and the work presented in it are my own. I confirm that:

i. The research reported in this thesis, except where otherwise indicated is my original work.

ii. This thesis has not been submitted for any degree or examination at any other university.

iii. This thesis does not contain any other persons' data, pictures, graphs or other information, unless specifically acknowledged as being sourced from other persons.

iv. This thesis does not contain other persons' writing, unless specifically acknowledged as being sourced from other researchers. Where other written sources have been quoted, then:

a) Their words have been re-written, but the general information attributed to them has been referenced;

b) Where their exact words have been used, their writing has been placed inside quotation marks, and referenced.

v. Where I have reproduced a publication of which I am author, co-author or editor, I have indicated in detail which part of the publication was actually written by myself alone and have fully referenced such publications.

vi. This thesis does not contain text, graphics or tables copied and pasted from the Internet, unless specifically acknowledged, and the source being detailed in the thesis and in the references sections.

Signed: Date: **22 March 2018**

DECLARATION 2

LIST OF PUBLICATIONS

Journal Publications

1. **Robson T. Reza,** and Viranjay M. Srivastava, "An empirical analysis of a six radio channel pseudo generator for better noise reduction in ranging systems" ***Far East J. of Electronics and Communications*** (*FJEC*), vol. 17, no. 6, pp. 1299-1307, Dec. 2017. (chapter 2 and chapter 4) ***[SCOPUS]***

2. **Robson T. Reza** and Viranjay M. Srivastava, "Improving cell tower geo-location using Quantum clock timing," ***Int. J. on Communications Antenna and Propagation*** *(IRECAP)*, vol. 8, no. x, pp. yy-zz, 2018, accepted. (chapter 2 and chapter 5) ***[SCOPUS]***

Conference Publications

3. **Robson T. Reza** and Viranjay M. Srivastava, "Effect of GSM Frequency Band on Received Signal Strength and Distance Estimation from Cell Tower," *10^{th} Int. Conf. on Developments in e-Systems Engineering (DeSE 2017)*, Paris, France, 14-16 June 2017, pp. 1-4, (chapter 3). ***[IEEE Xplore]***

DEDICATION

I dedicate this thesis to my parents who have stood by me for as long as I have known.

ACKNOWLEDGEMENTS

I would like express gratitude to my core supervisor Prof. (Dr.) Viranjay M. Srivastava for his unwavering support in my work. I would also like to forward my thanks to my colleagues and university staff for moral support and access to university resources. Lastly I would like to thank my family for the love and support.

ABSTRACT

The need of accurate passive (on demand) mobile geo-location technology has been a necessity in various fields i.e. emergency rescue services, location based advertising, vehicle tracking etc. This trend has been necessitated by two major driving forces firstly, Global Positioning Satellite (GPS) requires a constant line of sight to keep track of a device and second, the energy requirements for a constantly active GPS attach are too high to implement on mobile devices.

Mobile telecom companies have a vast footprint on major inhabited parts in the cities with which they can use to rollout a location service. Accurate cell tower geo-location opens a host of possibilities for example Location Based Services (LBS) like geographic marketing, emergency rescue services and navigation. However reliable location services have thus far only been confined to GPS because Radio Access Network (RAN), Universal Terrestrial Radio Access Network (UTRAN) and Evolved Universal Terrestrial Radio Access Network (E-UTRAN) faces various challenges when estimating distances by either propagation delay, received signal strength and timing techniques. This work is part of a push towards advancement of the location capabilities of radio networks to margins within the tolerance ranges of GPS. This work has analysis of various strategies that can be implemented to improve accuracy of geographic location using current network infrastructure. This research work looks to optimize current location technology by looking at:

1. The effect of frequency on Received Signal Strength (RSS) and distance estimation from cell tower (Chapter 3).

2. Introduction of orthogonal transmit channels for better noise reduction in distance estimates (Chapter 4).

3. Quantum timing on RAN for improved resolution in distance estimate (Chapter 5).

Simulations of different propagation and receive models has been implemented using the MATLAB design environment on typical radio channels with Gaussian noise to test each of the above-mentioned parameters. The results obtained have been used to test the theorem that better location algorithms and hardware can vastly improve mobile geo-location into GPS territory.

TABLE OF CONTENTS

LIST OF FIGURES

LIST OF TABLES

LIST OF ABBREVIATIONS

GPS	Global Positioning Satellite
LOS	Line Of Site
WCDMA	Wide-band Code Division Multiple Access
RAN	Radio Access Network
BSS	Base Station Sub-system
BTS	Base Transceiver Station
BSC	Base Station Controller
MSC	Mobile Switching Centre ()
TRX	Transceiver
VLR	Visitor Location Register
HLR	Home Location Register
MSISDN	Mobile Station International Subscriber Directory Number
IMSI	International Mobile Subscriber Identity
LAC	Location Area Code
LBS	Location based services
VAS	Value Added Services
OTT	Over The Top
RSS	Received Signal Strength
GSM	Global System for Mobile
UMTS	Universal Mobile Telecommunication Service
LTE	Long Term Evolution
NTP	Network Time Protocol
AoA	Angle of Arrival
TDoA	Time Difference of Arrival
ToA	Time of Arrival
ETDoA	Enhanced Time Difference of Arrival
RSCP	Received Signal Code Power
CPICH	Common Pilot Channel

BCCH	Broadcast Control Channel
FH	Frequency Hopping
SFH	Slow Frequency Hopping
ARFCN	Absolute Radio Frequency Number
FDMA	Frequency Division Multiple Access
QoS	Quality of Service
SNR	Signal to Noise Ratio
RMSE	Root Mean Square Error
SDH	Synchronous Digital Hierarchy
MTN	Microwave Transmission Network
TDMA	Time Division Multiple access
SDCCH	Standalone Dedicated Control Channel
FACCH	Fast-Associated Control Channel

CHAPTER 1

Introduction

1.1. Fundamentals of Geo-Location

Ever since the advent of mobility on the telecommunication platform, a whole new host of applications have evolved from the simple circuit switched voice call [1]. Handheld geo-location devices were first introduced in the United States of America in early *1970s* for use in military applications, this system came to be known as the Global Positioning Satellite (GPS) system. However, restrictions on civilian uses were later removed and GPS was made available for everyday use [2]. GPS makes use of geo-stationary satellites that orbit the planet to get a trilateral fix on the precise position of a handheld device. This approach uses Line of Site (LOS) broadcast because signals are sent in one direction from the satellite to the receiver, in other words its passive form of location based service [3].

The other approach that was developed for geo-location was cell tower triangulation. This approach used the same fundamentals that had been applied by the GPS pioneers but in this instance, the anchored reference points for the triangulation had become mobile tower cells [4, 5]. Unlike in the case of GPS, cell tower triangulation can be implemented by various means has been discussed in the following chapters.

1.2. Fundamentals of GSM and WCDMA

Due to the extensive nature of the GSM and Wide-band Code Division Multiple Access (WCDMA) infrastructure (Radio Access Network (RAN), Core Network, Packet data services), we shall only focus on the core network elements and the Base Station Sub-system (BSS). In Fig. 1.1, a comprehensive block diagram of a typical GSM network is presented.

In the GSM/2G architecture, each Base Transceiver Station (BTS) is controlled by a parent Base Station Controller (BSC). A BSC can control multiple BTSs that are specific to it. The Mobile Switching Centre (MSC) is the central signaling node for the network. Triangulation occurs on the Um-interface i.e. interface between the cell tower and the

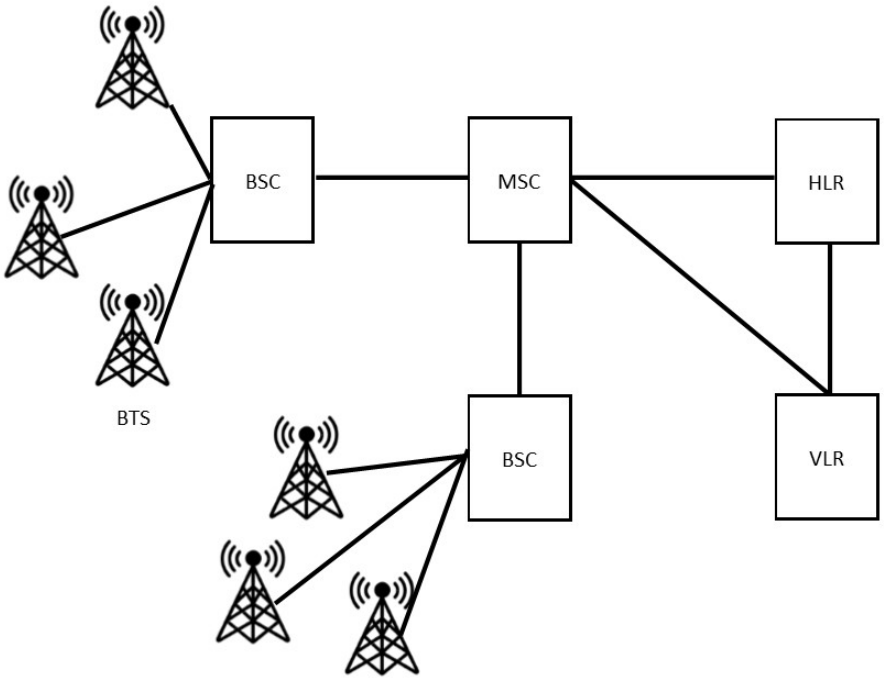

Figure 1.1. Simplified representation the GSM network.

mobile device. For better understanding of BTS and this wireless interface, we first need to have an appreciation of the cellular concept. In the cellular concept, the BTSs implement space division multiplexing. This is because they are positioned in different geographic locations. Each BTS covers a certain transmission area (cell). A cell is usually configured into *three* sectors, which are served by its own antenna as in Fig. 1.2.

A. *Base Station Controller (BSC)*

This network element controls multiple BTSs. Its main functions are:

- Performing radio resource management i.e. allocating transmission links to the various BTSs, allocating signaling and traffic channels via e-carrier links. It also allocates transceivers (TRXs) that are to be activated at sector level.
- Assigns and releases frequencies and time slots for all the mobile stations in its coverage area.
- Re-allocation of frequencies among cells.
- Hand over and cell reselection protocol is executed here.
- Time and frequency synchronization signals to BTSs.
- Time delay measurement and notification of an MS to BTS.
- Power Management of BTS and MS.

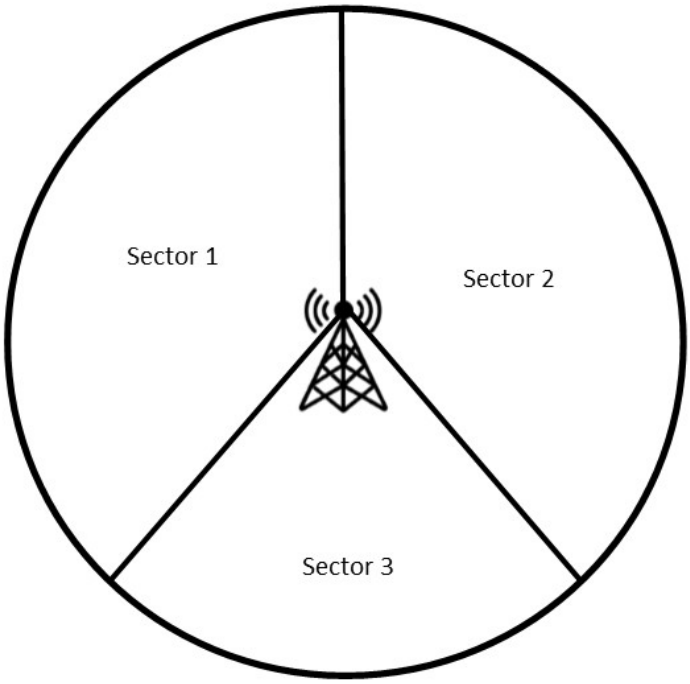

Figure 1.2. The cellular concept.

B. *Mobile Switching Centre (MSC)*

This is the switching point of all voice traffic in the mobile network. With later releases, the MSC no longer handles user traffic but is more of a media gateway controller. It is also responsible for inter-BSC handovers. The MSC subscriber mobility but making periodic location updates requests to the Visitor Location Register (VLR). The MSC handles call setup, conference calling, and call release measures.

C. *Home Location Register (HLR)*

This a central database where permanent subscriber information is stored. This includes:

- International Mobile Subscriber Identity (IMSI)
- Mobile Station International Subscriber Directory Number (MSISDN)
- Prepaid or postpaid status
- Roaming capabilities
- Subscriber authentication keys (KI encryption keys)
- Data capabilities

D. *Visitor Location Register (VLR)*

This is like a duplicate HLR, the main difference that the VLR exhibits is that is holds semi-permanent data like:

- Subscriber Location Area Code (LAC)
- Serving cell information
- Serving gateway information

1.3. Problem Definition

In the broad sense, tracking services are generally classified under Location-Based Services (LBS). Cell tower geo-location is used in various applications as stated below:

A. *Navigation* - Cellular devices can introduce new forms of passive car tracking that is not as accurate as GPS but can provide information like the general location of vehicles e.g. tracking a trucking fleet through a region or state.

B. *Emergency rescue services* - This feature is mostly applicable when a trauma victim dials 911 but cannot give an accurate location on his whereabouts hence cell tower location will be the best chance to locate that person.

C. *Advertising* - In this scenario, advertising content is sent to a potential customer based on his/her whereabouts e.g. if a subscriber roams into an area with a supermarket that has a certain item on promotion, then the network will send that subscriber an alert of that promotional item.

D. *Location based billing* - A mobile network provider can choose to employ different tariffs for different locations in order to promote a certain package to its subscribers

E. *Network analytics* - In the business work its essential to make informed decisions based on facts and current trends. With the ability to monitor the dynamic nature of mobile subscribers, it is easy to see a person's mobility patterns and hence improve the network, based on that information.

However, the main challenge with cellular based techniques in position location is the lack of precision and accuracy as compared to GPS [6-9]. *Yang et. al.* [10] have done extensive research to show that accuracy of cell tower triangulation can be improved by up to 80%. Most metro areas enjoy a large presence of mobile telecommunication

providers that have set up a large cell tower footprint that can be used for cell tower geolocation. GPS is the preferred location based service but it has its own fundamental flaws that cell tower triangulation can overcome. The GPS has two main challenges: (a) the device has high power consumption and (b) the receiver requires a line of sight i.e. no buildings and roofs. Cell tower geo-location methods are usually not free services and mobile telecommunication companies charge a fee for their use [11].

1.4. Motivation for the Work

The decision to work for 2G and partially 3G networks are due to following three main reasons:

A. *Power consumption and cell radius considerations* - LTE has been optimised for high data rates due to massive MIMO. However, use of LTE for range estimation would prove not ideal as device battery life will severely degrade in a very short space of time. Another issue is the issue of cell radius of LTE compared to cell radii for 2G, 2G can have cell radii of up to 3km whereas LTE shrinks down to a couple of hundred meters due to signal degradation on the radio interface with large distances.

B. *LTE and 4.5G penetration in emerging markets* - The candidate comes from one of the still emerging third world economies where adoption of 4G LTE services faces hindrances due to factors ranging from handset pricing constraints of devices that are LTE capable and where LTE coverage is not as pronounced as 2G and 3G. A good coverage profile is necessary for one to properly use a technology for location-based services.

C. *Trying to monetize the otherwise outdated voice switching* - Following the current trend from the Postal and Telecommunications Regulator of Zimbabwe (POTRAZ) 2017 quarterly report [1], voice has been on a steady decline due to Over-The-Top (OTT) services like WhatsApp and Twitter. 2G is mainly a circuit switching network and therefore with falling voice and SMS revenues there is need to find other uses of the now legacy technology for revenue generation.

Mobile telecommunication companies are currently facing a gradual decline in revenue due to the influence of Over The Top (OTT) services such as WhatsApp, Facebook, and Twitter etc. The 2017 *POTRAZ* report shows that the revenue for Zimbabwean mobile companies has declined by close to *9.7%* to a total of *179.8* million dollars, which translates to a decline of *19.3* million dollars. The worst affected was voice revenue that declined by *13.2%* in the quarter. This has made it apparent for the need to diversify revenue streams with Value Added Services (VAS). The least underutilized value-added service is passive location based services [12].

This work will also enable the use of location services in areas where it was previously not possible to get location information from GPS due to lack of line of sight e.g. inside buildings or in underground parking lots. Mobile network operators already have most of the required infrastructure needed to implement this new service to most of their subscribers. With reasonable capital injection and port monitoring on some of the core network nodes, it is possible to realize meaningful revenues and give better value to subscribers.

1.5. Objectives of This Research Work

This work intends to look at various ways to improve cell tower geo-location techniques to increase accuracy and reliability by improving current location techniques. This has been done by meeting certain predefined objectives that have been stated as follows:

A. Improve the current ranging techniques used in Received Signal Strength (RSS) by taking into consideration channel fading at varying Global System for Mobile (GSM) wavelengths.

B. Improve the current ranging techniques by creating orthogonal transmit channels (frequency diversity) to better mitigate against wavelength dependent fading and interference.

C. Improve the current ranging techniques by improving timing methods on the Radio Access Network (RAN) to improve resolution distances of cell tower triangulation. Models of quantum clocks have been used to simulate the output.

1.6. Contributions of Study

In current literatures, there is no any significantly noticeable study, which finds location information using mobile network infrastructure accurately. Great strides have been taken to advance other location techniques such as GPS. This study will add to the research that has already been done by *Forerunner's* in this field and will hopefully lead to implementation of this technology in other mainstream industries.

This study will add dimensions of band specific calculation to existing trilateration methods, band orthogonality (diversity) to triangulation and a completely new dimension of timing possibilities on RAN networks.

1.7. Organization of the Thesis

This present chapter introduces the topic of interest, the scope of the work to be covered and the motivation behind the work to be done. The objectives that are to be met are stated in this section.

Chapter 2 is divided into five distinct sections with the basic concepts that are used to implement trilateration and ranging estimation in GSM, Universal Mobile Telecommunication Service (UMTS) and Long-Term Evolution (LTE) networks. The section on geo-location techniques introduce the concept of the various techniques that have been implemented to archive location capabilities in mobile networks thus far. The comparison of GPS and cell tower triangulation section summarizes the findings of various studies that have been undertaken in the location based service industry when comparing GPS and cell tower triangulation.

Chapter 3 emphasizes the research work that improves the RSS based ranging algorithms based on frequency band. An analysis of the proposed model has been carried out and the results analyzed to ascertain the effectiveness of the proposed model.

Chapter 4 proposed a model to incorporate multi-channel diversity in the communication link to mitigate and reduce effects of frequency dependent fade and interference.

Chapter 5 outlines a proposed model, using a Network Time Protocol (NTP) server that is driven by an atomic clock to improve the performance of timing on the RAN when estimating the distance from mobile device. The results has been presented and

analyzed to find the impact of the proposed modifications to the accuracy of cell tower geo-location.

Finally, we conclude the thesis and recommend the future scope of the work in Chapter 6. It also includes the limitations of the work.

CHAPTER 2

Literature Review

2.1. Introduction

In this chapter we look at the various efforts and work that has been undertaken by previous authors, researchers, and scientists in localization using cell towers. The section looks at the major challenges that are faced with current generation location techniques and the approaches that have been used, thus far, to try to overcome them. Sources include various books, published journals and conference articles.

2.2. Cell Tower Geo-Location Techniques

The basic principle of the triangulation is to use the information provided by the network nodes to determine your position on a fixed grid. In Fig. 2.1, the mobile station is surrounded by base stations labelled as ***A***, ***B*** and ***C***. The handset estimates the distances r_1, r_2, and r_3 to find its approximate location in relation to ***A***, ***B*** and ***C*** using various techniques.

However, these techniques be it using Received Signal Strength (RSS), timing techniques or heuristic approaches always have noise factors that will affect readings and

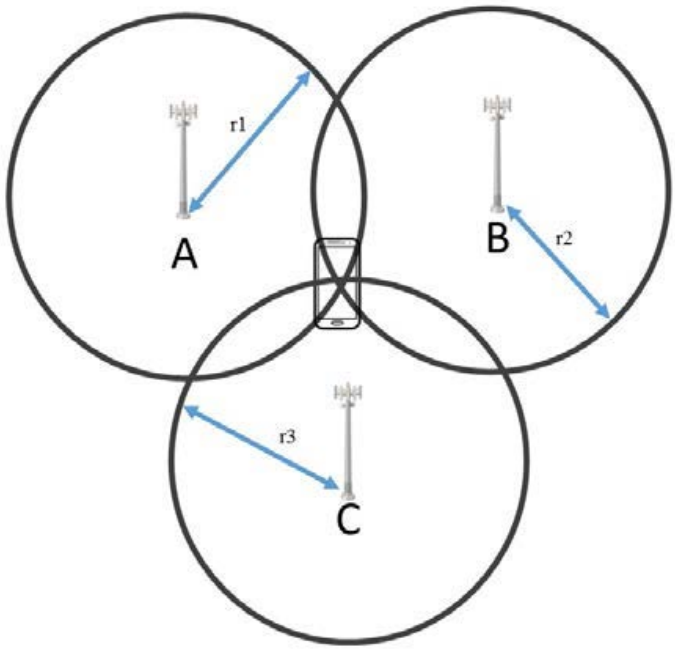

Figure 2.1. Simplified representation of cell tower triangulation.

thus the final point of intersection in the triangulation technique. Noise can either be random Gaussian or environment dependent and thus various algorithms have been devolved to reduce the effect of these noises [13, 14].

Cell tower geo-location techniques use various means to obtain the location of a handheld device. This can include the use of identifying tags such as cell identifiers (cell-ID), transceiver markers (TRX-ID), base station identifiers (BTS-ID), and Location Area Codes (LAC). However, approach that is more precise is the use of proximity sensing techniques like Angle of Arrival (AoA), Received Signal Strength (RSS) etc. Timing techniques that involve measuring the propagation delay between transmitter and receiver can also be implemented in the form of Time of Arrival (ToA), Time Difference of Arrival (TDoA) and Enhanced Time Difference of Arrival (ETDoA). Finally, a knowledge database can be created that will be superimposed on the geographic location and inference data is collected and mapped to the assumed position of the mobile device (Fingerprinting) [15-18].

The mobile triangulation falls under four broad categories: (i) Network based, (ii) Mobile based, (iii) Mobile assisted, and (iv) Network assisted. Fig. 2.2 shows two of the techniques and ways of implementing each.

Network based triangulation, is whereby a mobile network operator fully takes over the triangulation process to find a relative position of the subscriber using GSM, UMTS or LTE nodes. *Mobile based triangulation* is defined as the process that requires the handheld mobile device to calculate its location by utilizing measurement information provided by the network usually on the radio interface e.g. signal strength. A *network assisted approach* involves a process where the mobile calculates its location by taking network broadcast measurements and searching for its location by utilizing a mobile based approach with additional information supplied by the mobile network like Cell-IDs and Location Area Codes (LACs) on a network database. Finally, a *mobile assisted approach* is a technique where by it is purely a network-based triangulation that improves accuracy by taking in account information collected by the handheld device like neighbor cells and handover measurements [19]. In essence mobile-assisted and network-assisted techniques are in fact hybrids of pure network-based techniques or mobile-based techniques. Therefore, we have narrowed the field of vision of this work into the primary triangulation technologies that are available so as not to get side tracked

from the main goal. In the following sections we have discussed the mobile based and network-based techniques.

2.2.1. Network based approach

Uplink Time Difference of Arrival (U-TDoA): It estimates the position of a mobile station by measuring the time difference of arrival between the signals received at the serving cell and the same transmission received at an adjacent neighbor cell. By using at least three reference cells, a triangulation algorithm can be used to pin point the location of the mobile device by finding the intersection of the three hyperbolas formed by the ranging radii. To achieve a good result with this technique, precise time synchronization of the serving cells is a must.

Karl et. al. [20] have done extensive research in the field of U-TDoA and have published a work that compared the wireless and wired clock drift compensation. Timing accuracy, especially at the speeds of electromagnetic waves, requires that the clock on the transmitter and on the receiving device (in this case the phone) have to be precisely aligned. They specifically looked at Ultra Wide Band (UWB) IEEE 802.15.4 compliant devices that allow for time stamping of the transmitted data packets to and from the device.

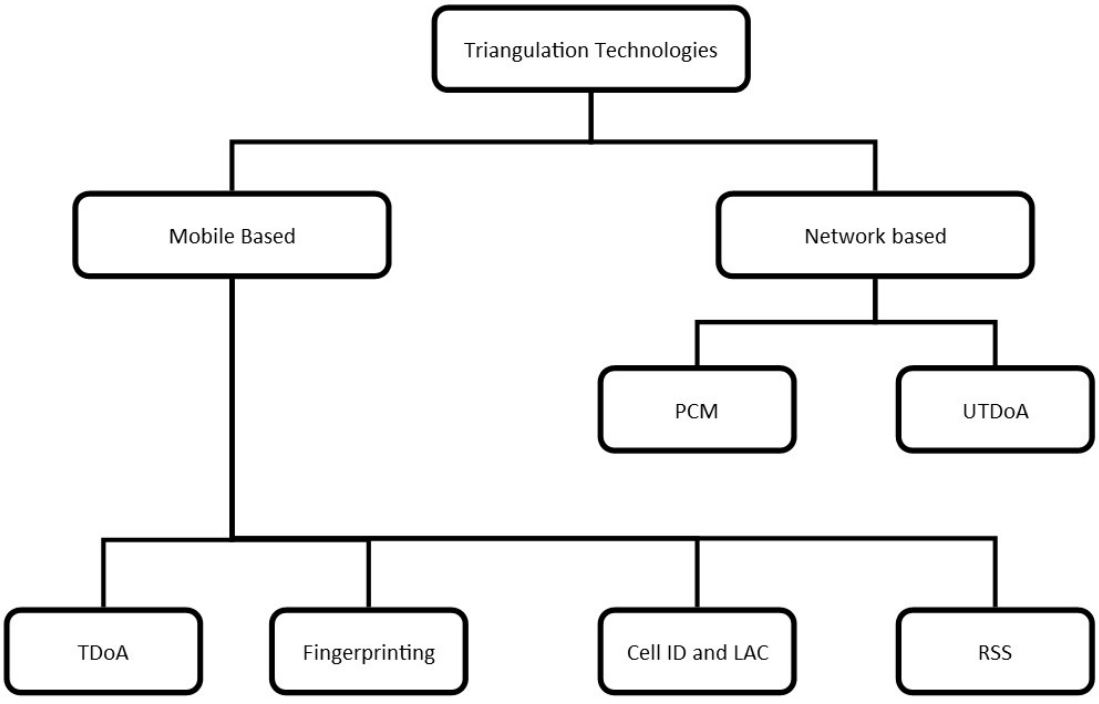

Figure 2.2. Breakdown of triangulation techniques.

The main trouble with U-TDoA is that there is always an element of clock drift between the two clocks. Methods have been devised to combat clock drift, mainly wired and wireless clock synchronization. After a certain period *T*, synchronization is required by the system:

$$T = \delta / x \tag{1}$$

where δ is the desired accuracy and x is the clock error in parts per million.

McElroy et. al. [21] have looked at the feasibility of using DW1000 transceivers, which are IEEE 802.15.4a compliant wireless devices on Wireless Sensor Networks (WSN) and are used in Real-Time Localization Systems (RTLS). They analyzed that, by decreasing the synchronization frequency between the anchors directly affected the accuracy of the triangulation technique.

Pilot Correlation Method (PCM): It utilizes the finger-printing. This is a purely network based location technique that is used in UMTS networks (3G), the geographic area is split into small manageable tracking areas. The mobile device measures the RSS from three or more sites i.e. Received Signal Code Power (RSCP) over the Common Pilot Channel (CPICH). This value is sent back to the network for triangulation.

Database Correlation Method (DCM) Fingerprinting: It has three categories, deterministic, probabilistic, and adaptive machine learning. Fingerprinting makes use of a heuristic approach of profiling a certain geographic area to come up with a location determining algorithm that when fed with certain information like RSS, AoA or TDoA the system can extrapolate a probable location of the device. Approaches like finger printing give better performance but they are exhaustive and difficult to scale up commercially [22].

Timing Techniques: Electromagnetic wave propagation is ideally equivalent to the speed of light in ideal conditions i.e. $3*10^8$ *m/s*. Without precise Timing and synchronization, the timing mechanisms of two remote devices will inevitably start to drift resulting in timing errors. A deviation in the order of *3.3 milliseconds* will directly result in a distance error in the order of kilometers. Generally, GPS is the superior geo-location technology because satellites use very precise timing from on-board cesium atomic clocks and at least two rubidium clocks. The GPS receiver calculates relative distances from a minimum of three satellites. These relative distances will be transformed into absolute three-dimensional coordinates and an absolute time coordinate.

Once off synchronization of a mobile device and a serving cell is not practical due to the fact of the inherent clock drift that will exist between two or more remote clocks [23]. It is also not feasible to prefabricate high accuracy low drift clocks in cellular devices due to the huge cost and technology implications. Various methods had been implemented that mitigate and to some extent remove issues of clock drift. These methods employ clock drift compensation either over a wireless or a wired interface [24]. There are two types of oscillators that can be used for implementation in clocks and timing circuits:

i. Use of atomic electron energy shifts (atomic) and crystal resonance.
ii. Quartz crystal oscillator (a circuit that is driven by the resonance of a thin film of quartz) to give a stable frequency [25-28].

An atomic oscillator is a circuit whose resonance frequency determined by energy shifts of valency electrons from high energy states to lower energy states. This is archived by passing the atom magnetic and microwave fields. In the example of a caesium *133 atom*, the electrons resonate at a frequency of *9.2 GHz* [29]. Most NTP servers run on atomic oscillators or they use GPS receivers [30, 31].

Time of Arrival Technique: The basic principle of network based triangulation is to use information provided by the mobile station to the respective adjacent network nodes (GSM/WCDMA/LTE) to determine the position of a transmitting device on a fixed grid [32-34]. In Fig. 2.3, the Mobile Station (MS) is in the middle of two cell towers labelled (x_1, y_1) and (x_2, y_2). The handset is at position (x_0, y_0) somewhere between the cell towers. The network infrastructure will calculate the distances d_1 and d_2 and will implement trilateration techniques to find the location of the handset. In Fig. 2.3, the distance between (x_0, y_0) and (x_1, y_1) is calculated using the coordinate system:

$$d_1 = \sqrt{\left(x_1 - x_0\right)^2 + \left(y_1 - y_0\right)^2} \tag{2.1}$$

$$d_2 = \sqrt{\left(x_2 - x_0\right)^2 + \left(y_2 - y_0\right)^2} \tag{2.2}$$

The time taken by the electromagnetic wave to travel this distance will be:

$$t = \frac{\left(\sqrt{\left(x_1 - x_0\right)^2 + \left(y_1 - y_0\right)^2}\right)}{c} \tag{2.3}$$

where c is the speed of light. These time values are very minute and precision timing is required to get the best results. There are factors that might affect propagation time estimates like signal degradation, multi path fading, no line of sight and most importantly low resolution with some of the timing clocks that is in use e.g. quartz crystal clocks hence the use of quantum clocks in GPS.

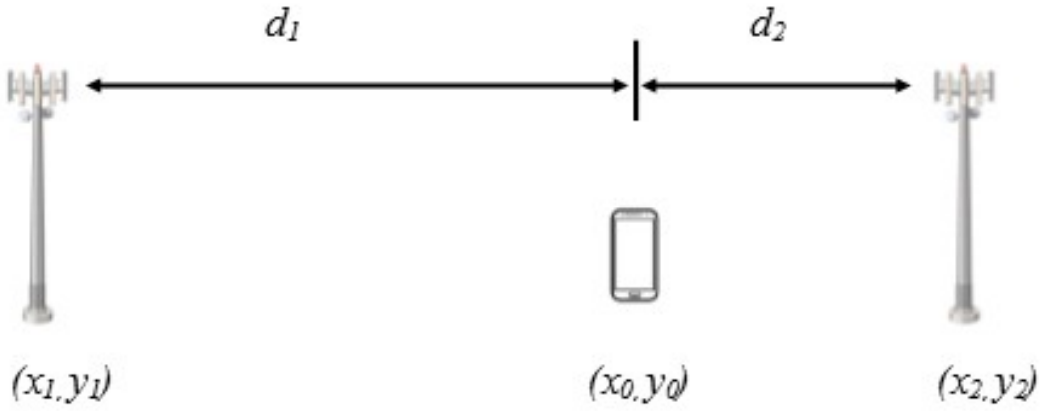

Figure 2.3. Simplified diagram of TOA.

Current Time Difference of Arrival (TDoA) techniques require those nodes (x_1, y_1) and (x_2, y_2) have precisely synchronised clocks so the distances d_1 and d_2 can be accurately determined. Synchronisation can be achieved by wired and wireless means. A better approach would be to synchronise the MS time with the time on the cell site and thereafter implement time difference techniques to improve ranging measurements. The estimate distance raw data is then sent to the network via network interfaces like the A-interface and Abis-interface. After that the geo-location trilateration calculations are handled by the network servers for further calculations by applying weighted algorithms.

2.2.2. Mobile based approach

This approach entirely relies on the handheld device to find a position estimate on a given geographic grid. An application will need to be installed on the device that will collect data fed to it by the network nodes.

RSS based ranging estimation: The simplest form of range estimation that was one of the pioneering methods was using RSS to estimate the distance between the cellular device and the BTS. Here a propagation loss and link budget equation would be used to predict attenuation as distance was increased between cell site and handheld device. Past ranging models have been based on the Friis transmission equation for simpler communication channel modelling and understanding. In attenuation-based simulations, the main components of fade are average path-loss, lognormal fading and small-scale fading. Although lognormal fading is not ideal when comparing with real world measurements it offers a sort of linear regression when modelling the distance and received signal strength [2].

Research work has been undertaken to compare the previously mentioned geo-location techniques. Simulations and data from field work have been analyzed. Combining two or more location techniques shows greater degrees of accuracy [35].

The RSS ranging hinges on the received signal intensity and gain properties on a receive antenna to try and establish and extrapolate a possible location of a device on a Cartesian plane [36]. In Fig. 2.1, the mobile station is surrounded by base stations labeled ***A***, ***B***, and ***C***. The handset estimates the distances r_1, r_2, and r_3 to find an approximate location using RSS algorithms. The mobile measures the receive level of the current attached channel and that on the BCCH for at least three base stations by sending an (AT+CSQ) command which returns values of the received signal strength. The mobile station then runs these RSS values in an algorithm to find a distance estimate from base station ***A***, ***B*** and ***C***. These distance estimates are then used to calculate the relative distance of each base station to the handset.

The transmitted signal loses power as distance from the transmitter increases and due to other factors like multi-path fading, shadowing, scattering and diffraction. To find the location of a mobile device the RSS characteristics of the mobile receiver, transmitter and frequency band should be known. The RSS values can be modeled by a constant component and a variable component [37]. Generally, the constant component is modeled by a path loss propagation model and the variable component is modeled by complex propagation effects like signal attenuation, shadowing, multipath, scattering, and diffraction [38]. In this section, the log normal shadowing model is used for modeling the RSS [39].

The variable component is modeled by the Friis transmission equation [40]. Eq. 2.4 is the Friis equation that can be re-written in logarithmic form to make received power:

$$P_r = P_t + G_t + G_r + 20\log_{10}\left(\frac{c}{4\pi fR}\right) \tag{2.4}$$

where *P* and *G* denote the power and gain respectively. *r* and *t* denote the receiver and transmitter, *f* , c, and R are the frequency, speed of light, and distance, respectively.

Channel hopping (Frequency diversity) based ranging estimation: Various research methods have looked at hybrids techniques to create better estimation models [41-43]. The main problem encountered when trying to find the fix of a mobile device is the unpredictability of the terrain where that technique is being implemented. A good example is of trying to triangulate in mountainous region, fade and multipath effects are severe. However, these effects are more pronounced for some frequency bands more than others. Fade is subdivided into two types:

a) Large scale fading - This is due to shadowing and mean path loss. This loss increases with distance between the transmit antenna and the receive antenna. Shadowing is signal attenuation due to obstacles in the path of the electromagnetic wave [44].

b) Small scale fading - This is responsible for the variation of RSS values by about 1%-2% of the actual value. Small scale fading is mainly due to factors like wave reflection, multipath, Doppler effects, flat fading and frequency selective fading as shown in Fig. 2.4 [45].

The basic assumption for signal strength in geo-location applications has been derived from the principles of applying a link budget approach to a wireless communication channel by taking into consideration antenna gains and power losses within the system. The Gaussian transmission channel can be described as the best-case scenario whereby the channel is only affected by adding white Gaussian noise at the receiver. Rayleigh channel is characterized by multi-path or scatter components that are

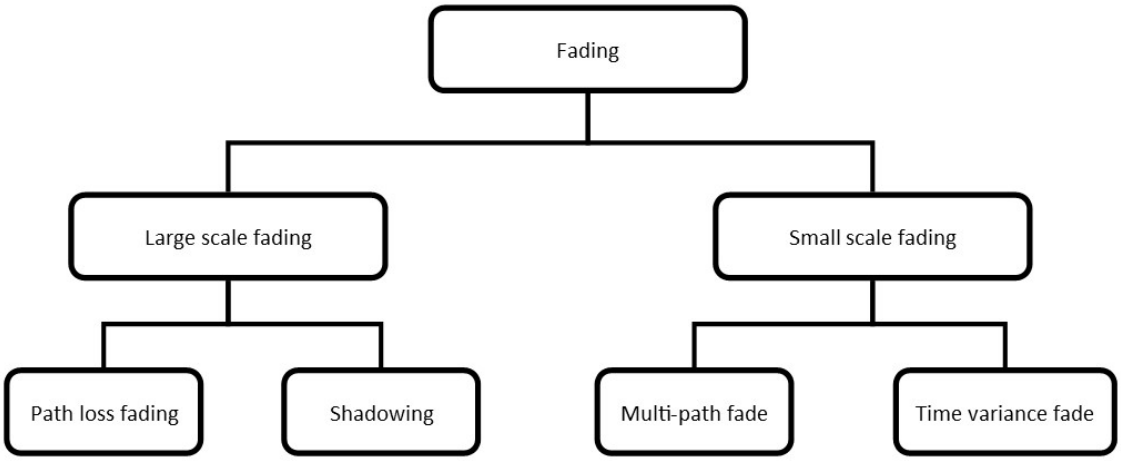

Figure 2.4. Types of fading.

received at the receiver. Various fading causes have been presented in Fig. 2.4. The *Rician channel* falls between the two extremes of an ideal *Gaussian channel* and the worst-case *Rayleigh channel* [45]. The Friis transmission equation does not give an exact representation of the actual link budget of a wireless system but instead offers a close model to the actual propagation channel. The amplitude of an electromagnetic wave is not only related to the inverse of frequency of transmission and distance between transmitter and receiver. The major cause of fading in urban environments is shadowing. Different electromagnetic wave frequencies penetrate buildings and encounter fading uniquely [47]. Therefore, if we had two separate channels that are uncorrelated frequency wise, then shadowing and attenuation will be likewise uncorrelated. There are two possible ways to mitigate random and unexpected fading effects that will otherwise affect RSS distance estimation.

a) Taking multiple RSS samples and finding the mean using the least squares regression method.

b) Splitting the transmit channel into multiple frequency channels that are uncorrelated and running the RSS distance algorithm on each channel then use the least squares regression method on the values of distance obtained. (Frequency diversity)

Diversity allows the rapid reduction in distance estimation error in wireless communications by creating several unique and independent transmission channels. Each of these channels will undergo its own fade and retardation characteristic. In the GSM communications, frequency diversity is implemented using Frequency Hopping (FH). The most common type of frequency hopping employed is Slow Frequency Hopping (SFH) whereby each carrier channel cycles through *64* predetermined frequencies. With each new symbol or burst, the logical channel changes for every *4.615 ms* [48].

Another approach to suppression of multipath and interference effects on received signal strength is with rake receivers. These work in third generation CDMA bands that have extended bandwidth for better time dispersive responses as opposed to the second-generation CDMA networks. A rake receiver is basically a modified antenna that does pulse sampling of the received signal through weighted fingers. These weights are calculated using a maximum likelihood formula. The generalized rake receiver gives gains of up to *3.5 dB* [49].

A rake receiver works on the principle of power taps, each tap has a delay function that will compensate for any received signal that that is received after it has been reflected on an object and thus has not taken a direct path from transmitter to receiver.

Fig. 2.5 shows the setup for a generalized rake receiver with two fingers, one tap captures the direct path *t* and the second tap captures the reflected waveform or multipath component t_r. The output is passed through an integrator which then goes into a logic adder (combiner) which will give the final output [50]. At the transmitter side, the transmitted symbol for user *k* can be expressed as:

$$x_k(t) = \sqrt{P_t} \sum_{i=-\infty}^{\infty} s_k(i) a_{k,i}(t - iT) \tag{2.5}$$

where P_t is the average symbol transmit energy, T is the symbol duration and $s_k(i)$ is the spreading symbol waveform. At the receiver assuming we have a collective of K users with L resolvable paths (fingers), then the signal will pass through an equivalent channel that has added white gaussian noise to give the following receive signal:

$$r(t) = \sum_{l=0}^{L-1} g_l x_0(t - T_l) + \sum_{k=1}^{K-1} \sum_{l=0}^{L-1} g_l x_k(t - T_l) + n(t) \tag{2.6}$$

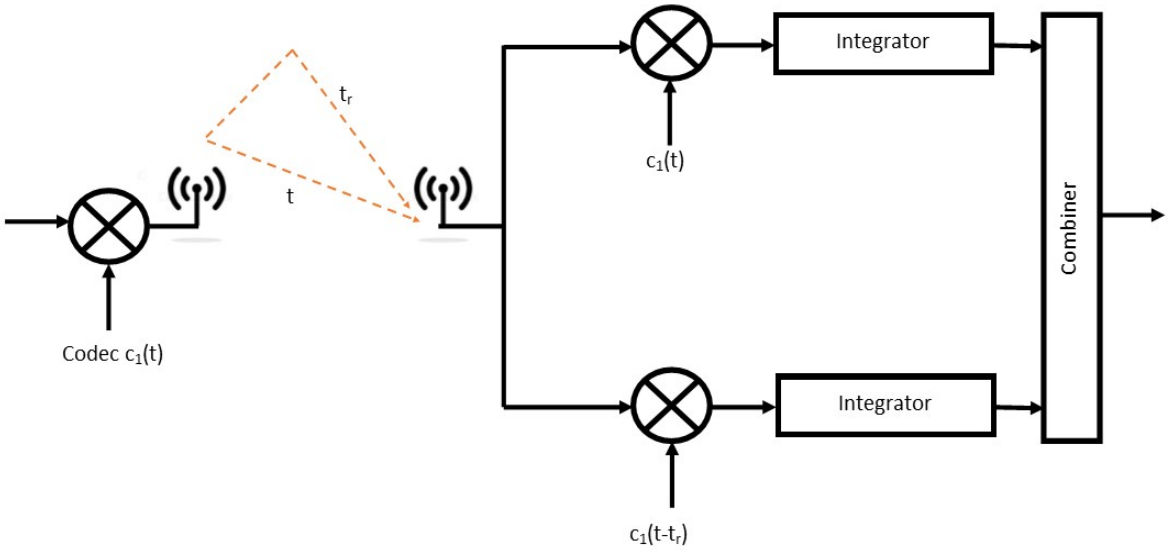

Figure 2.5. Rake receiver setup.

However, for our example we are assuming that we only have a single user therefore $K = 1$. The above expression simplifies to a simplified expression that only considers order of the rake receiver (number of resolvable paths) and channel noise as:

$$r(t) = \sum_{l=0}^{L-1} g_l x_0(t - T_l) + n(t) \tag{2.7}$$

Using this approach, rake receivers have used MRC to lower BER and improve communication systems. Fundamentally this approach can be used to single out peak amplitude impulses at the receiver end and ignore echo taps to mitigate multipath effects when calculating RSS values [51].

Enhanced Observed Time Difference (E-OTD) is the mobile based equivalent of the above-mentioned Uplink Time Difference of Arrival. The mobile device listens in on the broadcast channels from three or more sites to measure and record the time difference between the signals from the adjacent sites. It then either does a look up on an indexed database or uses offline maps to find its passion relatives to the sites [52].

Observed Time Difference of Arrival (OTDoA) system uses time difference measurements rather than absolute time measurements as TOA does. If the User Equipment (UE) is located at $x = (x_0, y_0)$ and the Node B stations at (x_i, y_i) where $i \in [1, 2, 3, \ldots N]$ then the distance between the Node B stations and the UE is given, by Eq. (2.1) and Eq. (2.2). Each pair of received measurements constrains the transmitter

position to a hyperbola along which the UE may be located. The intersection of at least two hyperbolas for several measurements determines the position of the different UEs. For this reason, this OTDoA technique is often referred to as the hyperbolic system and thus, the time difference is converted to a constant distance difference to two Node B stations (located at the foci) to define a hyperbolic curve [53].

$$d_1 - d_i = \sqrt{\left(x_1 - x_0\right)^2 + \left(y_1 - y_0\right)^2} - \sqrt{\left(x_i - x_0\right)^2 + \left(y_i - y_0\right)^2} \tag{2.8}$$

The time difference is therefore:

$$T_{DoA} = \left(d_1 - d_2\right) * c \tag{2.9}$$

where c is the speed of light.

Proximity sensing technique uses available network information like received signal strength, angle of arrival, cell ID and location area codes to find the approximate location of a mobile device. However, this could prove to be an inaccurate approach among the available forms of triangulation since broadcast cells can have radii of up to *3 km* in some instances where there is use of GSM 900.

2.2.3. Hybrid approach

In the hybrid approach, two or more methods of trilateration can be used to find the approximate position of a mobile device. This offers better performance than when each approach is used independently from the other. A localization algorithm is then formulated that will rely on a weighted centroid or least squares regression techniques. *Bishop et. al.* [54] used a hybrid approach of using Angle of Arrival (AoA) and TDoA in a geographically restricted area. They found that better performance was achievable than when compared to the systems being run in parallel.

2.3. Global Positioning System (GPS)

A GPS satellite transmits two data streams that are used to determine the position of the receiver at any given time i.e.:

a) Almanac, and

b) Ephemeris [55, 56].

The almanac contains relative information about the satellite itself, like is orbit and identity. The ephemeris gives an absolute fix on the position of the satellite and is used for trilateration in three dimensions to find the exact location of the receiver [57, 58]. A simplified diagram of the GPS setup is shown in Fig. 2.6. Generally, GPS is the superior geo-location technology because satellites use very precise timing from on board cesium atomic clocks and at least two rubidium clocks. Then the receiver calculates relative distances from a minimum of three satellites. These relative distances will be transformed into absolute three-dimensional coordinates and an absolute time coordinate. An atomic oscillator is a circuit whose resonance frequency determined by energy shifts of valence electrons from high energy states to lower energy states. This is achieved by passing the atom magnetic and microwave fields. In the example of a cesium *133* atom, the electrons resonate at a frequency of *9.2 GHz* [59]. Most NTP servers run on atomic oscillators or they use GPS receivers [60, 61].

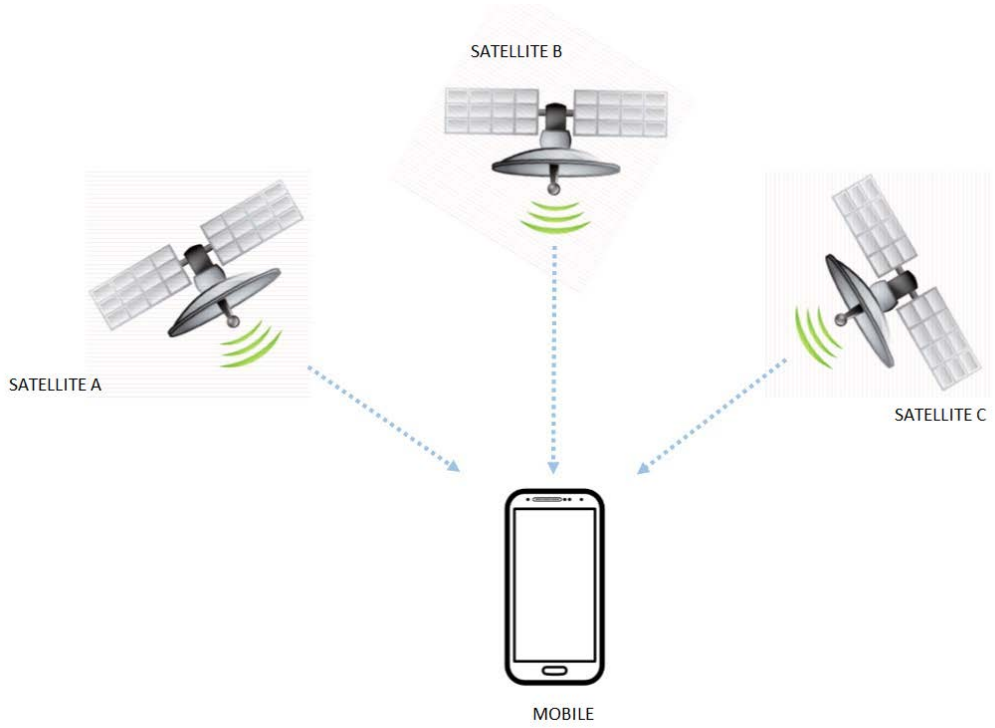

Figure 2.6. Simplified representation of GPS.

2.4. Comparison of GPS and Cell Tower Triangulation

A comparative analysis is essential for one to fully grasp the major differences, drawbacks and advantages that exist between location services based on GPS and cell tower triangulation. A full understanding of these will give a roadmap on how we can try to improve the accuracy and precision on cell tower location. We shall compare the cost of running the service, the coverage range of each technology, accuracy and real life applicability in terms of battery life and portability.

The pros and cons for both GPS and Cell tower location services has been summarized in Table 2.1 and Table 2.2. It is now clear to see that with the current technology, GPS is the superior positioning technology in use today [62].

From Table 2.1 GPS has the advantage of high location precision and a global coverage since it utilizes satellites to find a fix. However, GPS only works outdoors where there is a reliable line of sight with the satellites and has a high-power consumption. From table 2.2 its clear that cell tower has a clear disadvantage of coverage since it is only available where there is a mobile operator signal and also it is not precise when finding a fix of a mobile.

Table 2.1. GPS summary.

GPS Advantages	**GPS Disadvantages**
Free	Requires a line of sight
Available anywhere	Takes time to get initial fix
Relatively high precision	Relatively power-hungry devices

Table 2.2. Cell tower location summary.

Cell tower location Advantages	**Cell tower location Disadvantages**
Works anywhere there is cell reception	Is a charged service
Quick initial positioning	Not available globally
Relatively low power consumption	Requires high site density for accurate results
	Bad precision

2.5. Chapter Summary

It has been established without any doubt that although cell tower triangulation has seen some great advances and has many various techniques that can be used to implement it, there is still room for great improvement for this system to attain localization accuracy within the range of GPS.

Further chapters will now look at ways of mitigating the drawbacks of cell tower triangulation with specific focus on improving accuracy in finding a user location fix using this work.

CHAPTER 3
Improved RSS Based Ranging Using Band Specific Algorithm

3.1. Introduction

In this chapter, a new ranging method has been derived from fundamental RSS principles and simulated in MATLAB. The output results are then analyzed in order to come up with deductions of the proposed scheme. *Herald T. Friis* presented an equation that modelled the transmission path of an electromagnetic wave in 1946. This was related to the distance between transmitter and receiver with the wavelength and transmit power. This came to be known as the Friis transmission equation. We will be looking at a model that uses a modified version of this equation in RSS triangulation.

3.2. Modeling of Structure

The current RSS based models are somewhat unreliable, mainly because the GSM has various bands in which it can work. Each of these bands operates with distinct uplink and downlink frequencies. Each band therefore has its own unique fade response and interference susceptibility. Thus, a global ranging algorithm is not ideal when trying to find approximate location based on RSS values [53, 63-65].

Table 3.1. GSM frequency bands [66].

Bands	ARFCN	Uplink (MHz)	Downlink (MHz)
GSM 900 (primary)	0–124	890–915	935–960
GSM 900 (extended)	975–1023, 0–124	880–915	925–960
GSM 1800	512–885	1710–1785	1805–1880
GSM 1900	512–810	1850–1910	1930–1990
GSM 850	128–251	824–849	869–894
GSM-R	0–124, 955–1023	876–915	921–960

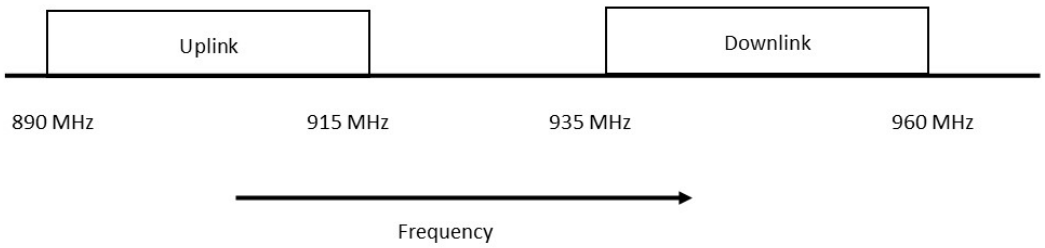

Figure 3.1. GSM 900 band.

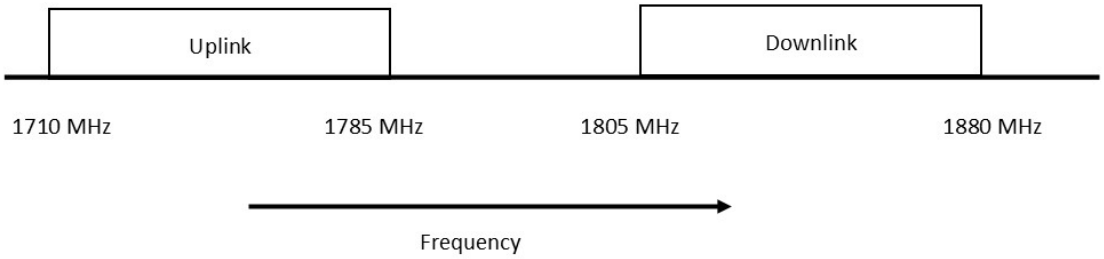

Figure 3.2. GSM 1800 band.

The GSM *900 MHz* band is used in instances where coverage distance is a priority rather than subscriber density and the higher bands i.e. GSM *1800 MHz* are used in metropolitan areas where there is high customer and network density. The GSM *900 MHz* uplink has a bandwidth of 25*MHz* and it is split into 125 sub-channels each with a *200 kHz* size, in Fig. 3.1. The GSM *1800 MHz* uplink has a bandwidth of *75 MHz* and it is split into *500* sub-channels each with a *200 kHz* size, in Fig. 3.2 [67].

The GSM has six frequency bands that are in use, each of these frequencies is applied to the Friis propagation model Eq. (3.1) and corresponding data of the RSS characteristics of the received signal logged. The downlink frequency band is split into five equal segments from *920 MHz* to *1990 MHz* to find the attenuation response over the range:

$$P_r = P_t + G_t + G_r + 20\log_{10}\left(\frac{c}{4\pi fR}\right) \tag{3.1}$$

Table 3.2 shows the initial conditions that were plugged in the model. The receive distance was kept constant and the frequency is varied over the range in Table 3.2.

Table 3.2. Initial conditions.

	Value
BTS transmit power	30 dB
Gain of the transmitter	5 dB
Gain of the receiver	2 dB
Frequency range	920 MHz-1990 Mhz
Distance range	50 m-5000 m
Speed of light	$3*10^8$

3.3. Simulation and Results of the Model

For each of the test frequency block, one hundred samples are taken of the RSS values at each distinct displacement interval between the cell tower and the mobile device. This is repeated for five different frequency bands. Typical output values are shown in listed in Table 3.3 the mathematical model is shown in appendix A.

Next to measure the scatter of the data that was obtained, the standard deviation of the data was calculated as shown below [68].

$$SD = \sqrt{\frac{\sum (d - \mu)^2}{n}} \tag{3.2}$$

where d is the distance estimate, is the mean of the sample and n is the number of samples.

Fig. 3.3 shows the data from Table 3.3 after being plotted. The measured distance was placed on the x-axis vs received signal power on the y-axis. Fig. 3.4 shows the deviation that is caused by the change in band when receive distance is maintained. The data from the bar graph was obtained from values in Table 3.3. The frequency of the transmit signal has been plotted on the x-axis and the measured distance is plotted on the y-axis.

Varying the frequency and distance was done in order to come up with a usage profile for a user in motion and experiencing frequency reselection either due to soft handover or hard handover.

Table 3.3. RSS values for five specific GSM frequencies with varying distance.

Distance (m)	RSS_1 (dB)	RSS_2 (dB)	RSS_3 (dB)	RSS_4 (dB)	RSS_5 (dB)
50	-28.69692882	-30.91384464	-32.67843214	-34.14435688	-35.3982338
100	-34.71752873	-36.93444455	-38.69903205	-40.1649568	-41.41883371
150	-38.23935391	-40.45626973	-42.22085723	-43.68678198	-44.9406589
200	-40.73812865	-42.95504447	-44.71963197	-46.18555671	-47.43943363
250	-42.67632891	-44.89324473	-46.65783223	-48.12375697	-49.37763389
300	-44.25995383	-46.47686965	-48.24145715	-49.70738189	-50.96125881
350	-45.59888962	-47.81580544	-49.58039294	-51.04631768	-52.3001946
400	-46.75872856	-48.97564438	-50.74023188	-52.20615662	-53.46003354
450	-47.78177901	-49.99869483	-51.76328233	-53.22920707	-54.48308399
500	-48.69692882	-50.91384464	-52.67843214	-54.14435688	-55.3982338
550	-49.52478252	-51.74169834	-53.50628584	-54.97221059	-56.2260875
600	-50.28055374	-52.49746956	-54.26205706	-55.72798181	-56.98185872
650	-50.97579587	-53.19271168	-54.95729919	-56.42322393	-57.67710085
700	-51.61948953	-53.83640535	-55.60099285	-57.0669176	-58.32079451
750	-52.218754	-54.43566982	-56.20025732	-57.66618207	-58.92005898
800	-52.77932847	-54.99624429	-56.76083179	-58.22675654	-59.48063345
850	-53.30590725	-55.52282307	-57.28741057	-58.75333531	-60.00721223
900	-53.80237892	-56.01929474	-57.78388224	-59.24980699	-60.5036839
950	-54.27200084	-56.48891666	-58.25350416	-59.7194289	-60.97330582
1000	-54.71752873	-56.93444455	-58.69903205	-60.1649568	-61.41883371
1050	-55.14131471	-57.35823053	-59.12281803	-60.58874278	-61.8426197
1100	-55.54538244	-57.76229826	-59.52688576	-60.9928105	-62.24668742
1150	-55.93148554	-58.14840136	-59.91298886	-61.3789136	-62.63279052
1200	-56.30115365	-58.51806947	-60.28265697	-61.74858172	-63.00245864
1250	-56.65572899	-58.87264481	-60.63723231	-62.10315706	-63.35703397
1300	-56.99639578	-59.2133116	-60.9778991	-62.44382384	-63.69770076
1350	-57.3242041	-59.54111992	-61.30570742	-62.77163217	-64.02550908
1400	-57.64008945	-59.85700527	-61.62159277	-63.08751751	-64.34139443
1450	-57.94488878	-60.1618046	-61.9263921	-63.39231684	-64.64619376
1500	-58.23935391	-60.45626973	-62.22085723	-63.68678198	-64.9406589
1550	-58.5241627	-60.74107852	-62.50566602	-63.97159076	-65.22546768
1600	-58.79992839	-61.01684421	-62.78143171	-64.24735645	-65.50123337
1650	-59.06720762	-61.28412344	-63.04871094	-64.51463568	-65.7685126
1700	-59.32650716	-61.54342298	-63.30801048	-64.77393523	-66.02781214
1750	-59.57828971	-61.79520553	-63.55979303	-65.02571777	-66.27959469
1800	-59.82297884	-62.03989465	-63.80448215	-65.2704069	-66.52428382
1850	-60.0609633	-62.27787912	-64.04246662	-65.50839137	-66.76226828
1900	-60.29260075	-62.50951657	-64.27410407	-65.74002882	-66.99390573
1950	-60.51822096	-62.73513678	-64.49972428	-65.96564902	-67.21952594

2000	-60.73812865	-62.95504447	-64.71963197	-66.18555671	-67.43943363
2050	-60.95260595	-63.16952177	-64.93410927	-66.40003402	-67.65391094
2100	-61.16191463	-63.37883045	-65.14341795	-66.60934269	-67.86321961
2150	-61.36629793	-63.58321375	-65.34780125	-66.813726	-68.06760291
2200	-61.56598235	-63.78289817	-65.54748567	-67.01341041	-68.26728733
2250	-61.7611791	-63.97809491	-65.74268241	-67.20860716	-68.46248408
2300	-61.95208545	-64.16900127	-65.93358877	-67.39951352	-68.65339043
2350	-62.13888598	-64.3558018	-66.1203893	-67.58631404	-68.84019096
2400	-62.32175357	-64.53866939	-66.30325689	-67.76918163	-69.02305855
2450	-62.50085042	-64.71776624	-66.48235374	-67.94827848	-69.2021554
2500	-62.67632891	-64.89324473	-66.65783223	-68.12375697	-69.37763389
2550	-62.84833234	-65.06524816	-66.82983566	-68.29576041	-69.54963732
2600	-63.01699569	-65.23391151	-66.99849901	-68.46442376	-69.71830067
2650	-63.18244621	-65.39936203	-67.16394953	-68.62987428	-69.88375119
2700	-63.34480402	-65.56171984	-67.32630734	-68.79223208	-70.046109
2750	-63.50418261	-65.72109843	-67.48568593	-68.95161067	-70.20548759
2800	-63.66068936	-65.87760518	-67.64219268	-69.10811742	-70.36199434
2850	-63.81442593	-66.03134175	-67.79592925	-69.261854	-70.51573091
2900	-63.96548869	-66.18240451	-67.94699201	-69.41291676	-70.66679367
2950	-64.11396905	-66.33088487	-68.09547237	-69.56139712	-70.81527403
3000	-64.25995383	-66.47686965	-68.24145715	-69.70738189	-70.96125881
3050	-64.40352552	-66.62044134	-68.38502884	-69.85095358	-71.1048305
3100	-64.54476261	-66.76167843	-68.52626593	-69.99219067	-71.24606759
3150	-64.68373981	-66.90065563	-68.66524313	-70.13116787	-71.38504479
3200	-64.8205283	-67.03744412	-68.80203162	-70.26795636	-71.52183328
3250	-64.95519595	-67.17211177	-68.93669927	-70.40262402	-71.65650093
3300	-65.08780753	-67.30472335	-69.06931085	-70.5352356	-71.78911251
3350	-65.21842487	-67.43534069	-69.19992819	-70.66585294	-71.91972985
3400	-65.34710707	-67.56402289	-69.32861039	-70.79453514	-72.04841206
3450	-65.47391063	-67.69082645	-69.45541395	-70.9213387	-72.17521562
3500	-65.59888962	-67.81580544	-69.58039294	-71.04631768	-72.3001946
3550	-65.72209579	-67.93901161	-69.70359911	-71.16952386	-72.42340078
3600	-65.84357875	-68.06049457	-69.82508207	-71.29100681	-72.54488373
3650	-65.96338602	-68.18030184	-69.94488934	-71.41081409	-72.664691
3700	-66.08156321	-68.29847903	-70.06306653	-71.52899128	-72.7828682
3750	-66.19815409	-68.41506991	-70.17965741	-71.64558215	-72.89945907
3800	-66.31320067	-68.53011648	-70.29470398	-71.76062873	-73.01450565
3850	-66.42674332	-68.64365914	-70.40824664	-71.87417139	-73.1280483
3900	-66.53882087	-68.75573669	-70.52032419	-71.98624894	-73.24012585
3950	-66.64947065	-68.86638646	-70.63097397	-72.09689871	-73.35077563
4000	-66.75872856	-68.97564438	-70.74023188	-72.20615662	-73.46003354
4050	-66.8666292	-69.08354502	-70.84813252	-72.31405726	-73.56793418
4100	-66.97320587	-69.19012169	-70.95470919	-72.42063393	-73.67451085

4150	-67.07849067	-69.29540649	-71.05999399	-72.52591873	-73.77979565
4200	-67.18251454	-69.39943036	-71.16401786	-72.62994261	-73.88381952
4250	-67.28530733	-69.50222315	-71.26681065	-72.7327354	-73.98661232
4300	-67.38689784	-69.60381366	-71.36840116	-72.83432591	-74.08820283
4350	-67.48731387	-69.70422969	-71.46881719	-72.93474194	-74.18861885
4400	-67.58658226	-69.80349808	-71.56808558	-73.03401033	-74.28788724
4450	-67.68472895	-69.90164477	-71.66623227	-73.13215702	-74.38603393
4500	-67.78177901	-69.99869483	-71.76328233	-73.22920707	-74.48308399
4550	-67.87775667	-70.09467249	-71.85925999	-73.32518473	-74.57906165
4600	-67.97268537	-70.18960119	-71.95418869	-73.42011343	-74.67399035
4650	-68.06658779	-70.28350361	-72.04809111	-73.51401586	-74.76789277
4700	-68.15948589	-70.37640171	-72.14098921	-73.60691396	-74.86079087
4750	-68.25140093	-70.46831674	-72.23290424	-73.69882899	-74.95270591
4800	-68.34235348	-70.5592693	-72.3238568	-73.78978155	-75.04365846
4850	-68.43236351	-70.64927932	-72.41386682	-73.87979157	-75.13366849
4900	-68.52145033	-70.73836615	-72.50295365	-73.9688784	-75.22275531
4950	-68.60963271	-70.82654853	-72.59113603	-74.05706078	-75.31093769
5000	-68.69692882	-70.91384464	-72.67843214	-74.14435688	-75.3982338

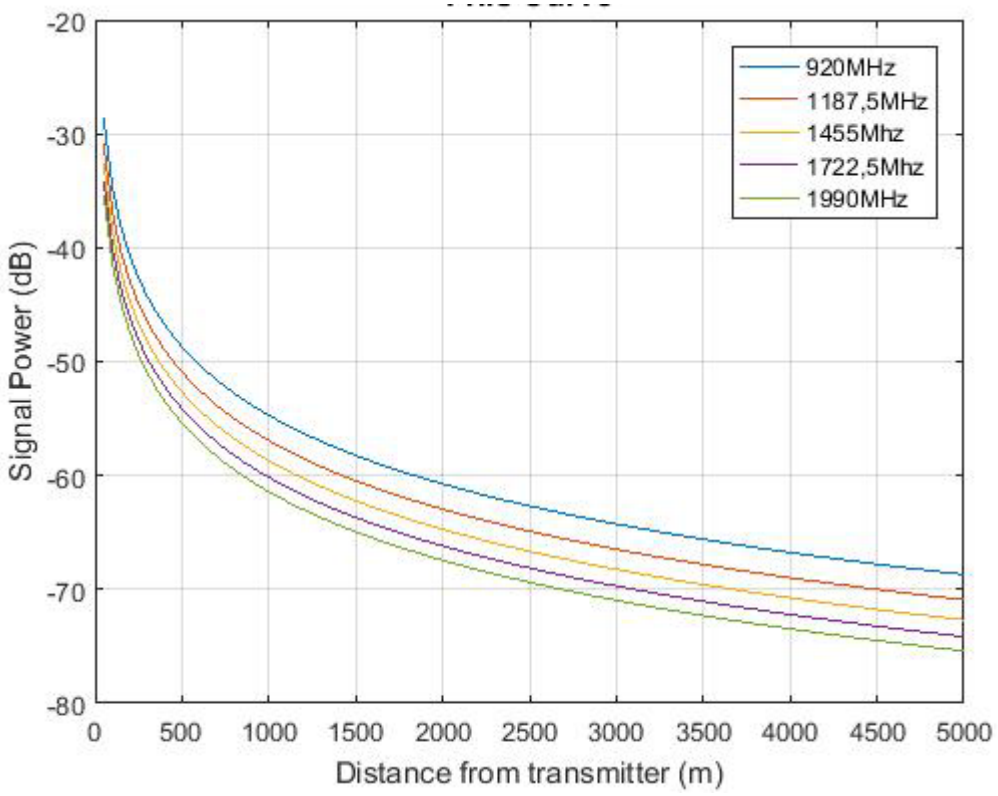

Figure 3.3. Signal attenuation with changing frequency.

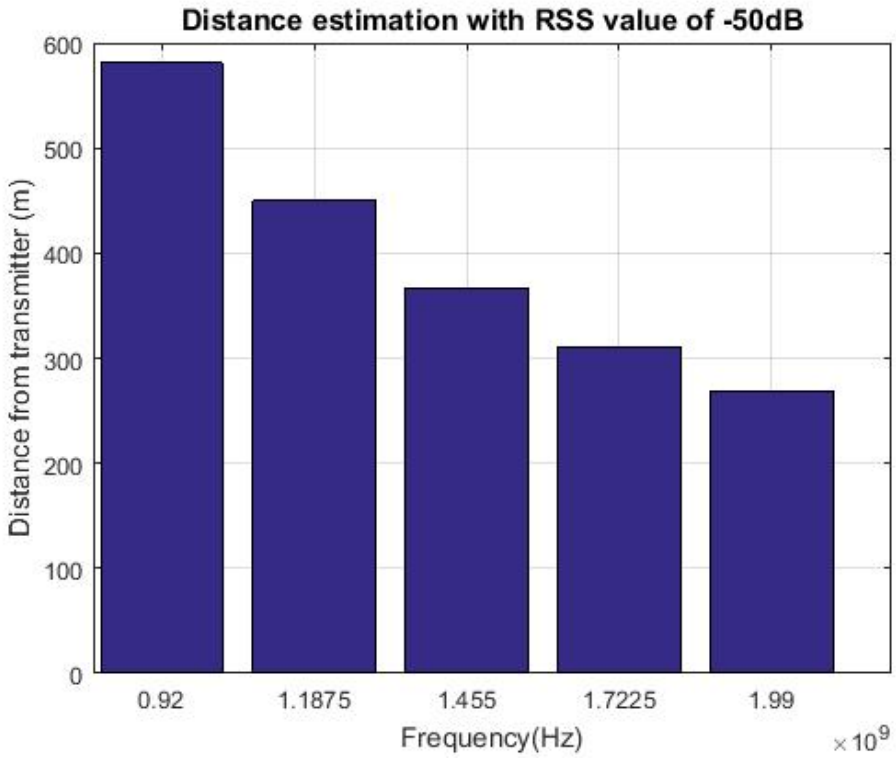

Figure 3.4. Actual distance with varying frequency.

3.4. Analysis of the Proposed Model

Simulation results show how a change of downlink frequency affect the distance estimation that the mobile would calculate if it only used RSS values for location without putting into consideration the band which the phone was latched on to. An RSS value of *-50 dB* is obtained at different distances from the transmitter depending on which band the mobile is fixed on as shown in Fig. 3.4. In the *920 MHz* band this RSS value is received at *581 meters* but in the *1990 MHz* band it is received at *268 meters*. Analysis of the data obtained from simulation shows that as frequency increases, RSS values change as well.

With a fixed RSS value of *-50 dB* the estimated differences differ with a standard deviation of *124 meters* for each frequency. A modified ranging equation was derived from the standard Friis equation that can accurately position a mobile device based on the attached frequency band.

This new equation will have a constant of proportionality *k* that varies with frequency, rearranging the Eq. (3.1) gives rise to the expression:

$$P_r - P_t - G_t - G_r = \log_{10}\left(\frac{c}{4\pi fR}\right)^{20} \tag{3.3}$$

This can be simplified to make the expression containing the distance R:

$$\sqrt[20]{10^{(P_r - P_t - G_r - G_t)}} = \left(\frac{c}{4\pi fR}\right) \tag{3.4}$$

If we are to assume that the distance *R* is held constant and the transmit/receive properties of the antenna are unchanged, then the change in receive signal strength will be accounted for with the change in frequency band. This change can be represented as:

$$R \ \alpha \ \frac{1}{f}$$

So,

$$R = k\left(\frac{1}{f}\right)$$

A new distance equation for use in cell tower triangulation based on RSS has been obtained as:

$$R = \frac{c}{4\pi kf\left(\sqrt[20]{10^{(P_r - P_t - G_r - G_t)}}\right)} \tag{3.5}$$

where values of *k* for each frequency are given in Table 3.4. Each value of *k* is for a specific frequency and this principle can be extrapolated by the use of curve fitting on graphs in figure 3.3 to adapt to any frequency. The main point that was trying to be put across here was that values of *k* should be calculated for any frequency band.

Equation (3.5) is now the modified version of the Friis transmission equation where we have factored a constant of proportionality *k* that is dependent on transmit wavelength. Table 3.4 shows the corresponding value of *k* for each transmits frequency. As the frequency increases, the value of *k* increases

Table 3.4. Calculated values of *k*

Sr. No.	Frequency (MHz)	*k*
1	920	1
2	1187.5	0.7747
3	1455	0.6323
4	1722.5	0.5341
5	1990	0.4623

3.5. Chapter Summary

From the above simulation and result data it is clear to see just how frequency factors in ranging accuracy when in use in triangulation applications. A value *k* needs to be factored in the ranging calculation to ensure accurate ranging results. The magnitude of *k* will vary depending on the band in question.

This chapter has shown that definitive improvements can be made if the trilateration application can factor in the baseband frequency of either GSM 900 MHz, GSM 1800 or the extended range of GSM. Further variables can be added in the modified equation like terrain and geographic overlay.

CHAPTER 4
Improved RSS Based Ranging Using Orthogonal Transmit Channels

4.1. Introduction

In the previous chapter (Chapter 3) we have identified some of the limitations that comes with RSS based ranging techniques. In this chapter we introduce a new aspect in RSS ranging by means of adapting our antenna to support frequency diversity schemes and find a mean RSS value that will be used to make a range estimate.

In this section we focus on way of mitigating channel specific fade by means of implementing a diversity scheme that has already been incorporated in the GSM architecture in the form of frequency hopping. A hopping sequence has been initiated within a specific band using baseband frequency hopping.

4.2. Orthogonal Transit Channel Model

The GSM standard allows for the use of multiple channels when communicating with a single device. The GSM burst or frame is structured as shown in Fig. 4.1. GSM operates by using Time Division Multiple Access (TDMA) over an assigned frequency range. A transmit packet is called a GSM burst and each burst is split into *eight* timeslots. Time slot is a complete virtual container that can carry the payload and integrate interference protection by use of guard bands.

To have a better visualization of how each TDMA frame translates into a channel on a TRX, the respective time slots are stacked in a vertical manner as shown in Fig. 4.2. A parameter in the BSC is the defined that is known as ALL_FHOP, this command enables the frequency-hopping algorithm. A TRX now can change its uplink and downlink frequency within a fixed frequency range of assigned an ARFCN. Each TRX is now implementing frequency diversity for a single session.

During the first transmit cycle, timeslot *one* transmits uplink data on frequency f_1 and the downlink frequency will be f_2. In the next timeslot, the TRX then utilizes frequencies f_3 and f_4 for its uplink and downlink respectively.

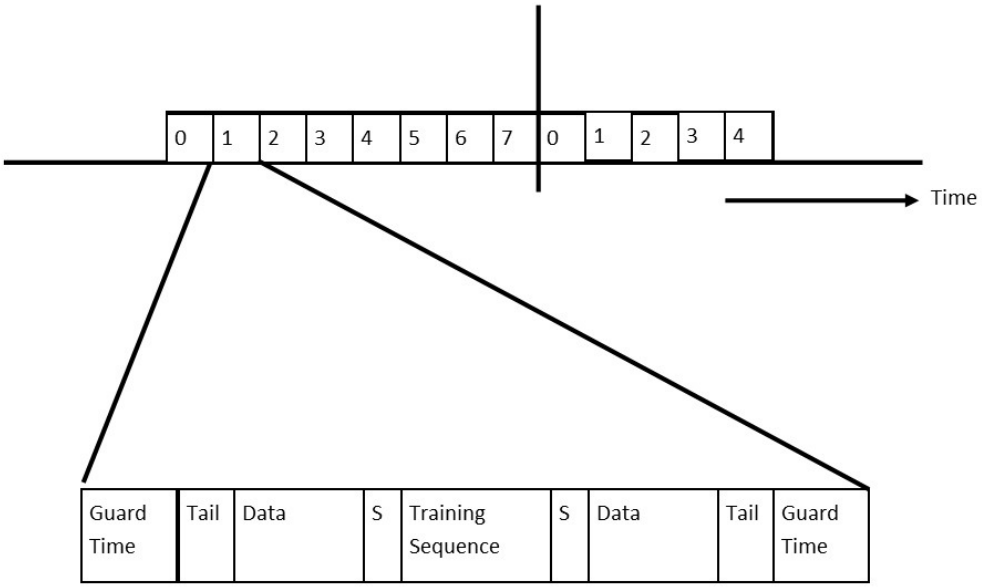

Figure 4.1. GSM Burst.

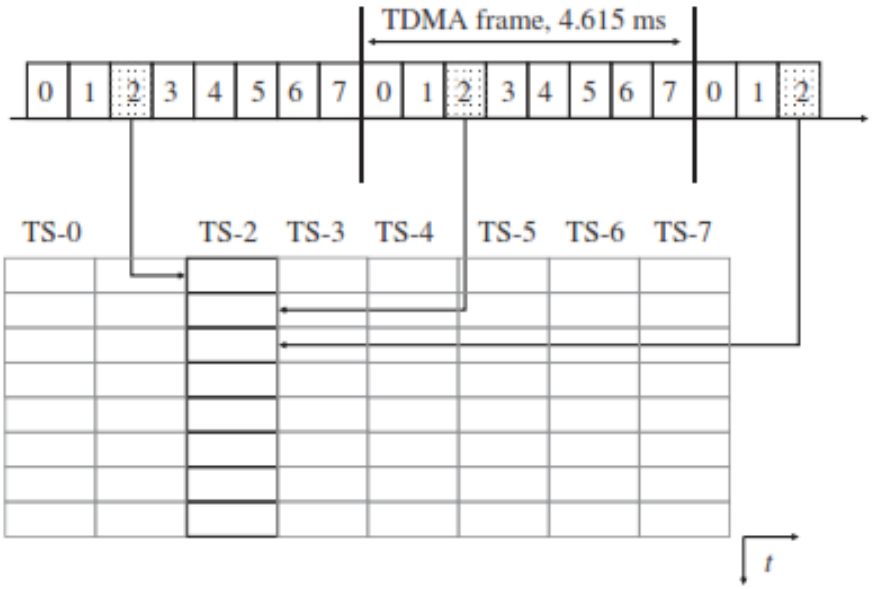

Figure 4.2. GSM logical channel representation [69].

A BSC will utilize this frequency hopping technique to mitigate the effects of channels specific fade and thus achieve uniform Quality of Service (QoS). Starting from an elementary single carrier system model, where we have a transmitted symbol {S_m} and the symbol period is T. This symbol will be transmitted through a channel *h(t)* after going through a transmit filter *gT(t)* where additive noise will be introduced *n(t)*.

Antenna at the receiver will take the received symbol through a receive filter $g_R(t)$ and equalizer $h\text{-}1(t)$ [48]. The signal recovered at the receiver $y(t)$ is:

$$y(t) = \sum_{m}^{\infty} s_m g(t - mT) + n(t) \tag{4.1}$$

where

$$g(t) = g_T(t) * h(t) * g_R(t) * h^{-1}(t) \tag{4.2}$$

To ensure that this channel is indeed frequency non-selective, the symbol period should be way greater than ten times the delay spread of Sm at the receiver ($T >> 10$). At the detector side, a modified path loss algorithm is run that includes shadowing, random power noise and the frequency component of fading to create the RSS receive matrix where each row is an independent frequency channel. The RSS value derived from the Friis transmission equation P_r is given shown as:

$$P_r = P_t + G_t + G_r + 20\log_{10}\left(\frac{c}{4\pi fR}\right) + n(0, N) - P_s \tag{4.3}$$

The P_t and P_s are the antenna transmit power and power loss due to shadowing, respectively and c, f, and R are the speed of light, frequency of the electromagnetic wave and distance between receiver and transmitter, respectively. The SNR will be determined by n, which is white Gaussian random noise that is normally distributed (multipath effects and interference). To simulate a noisy channel, $n(0,N)$ is initially set to a high value and gradually lowered to zero. A reception matrix of P_r values with dimensions (n x m) will store incoming RSS values. The rows, n represent the number of transmit frequencies and m is the RSS value at each sample period. Fig. 4.3 shows the logical block diagram of the diversity technique.

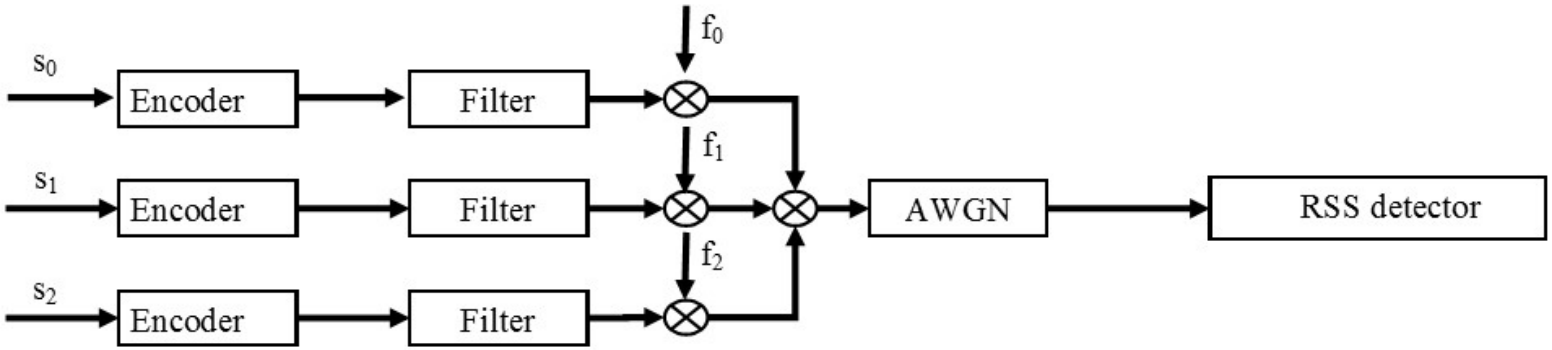

Figure 4.3. Model for multi-channel RSS trilateration with advantage of frequency non-selective fade.

Assuming F is the frequency matrix represented as $F = [F_1, F_2, F_3 \ldots\ldots F_n]$. The F matrix has been iterated through the range estimating equation and each iteration affected by a scaling constant k that is dependent on the frequency [70].

$$P_r = \begin{pmatrix} Rss_{11} & \cdots & Rss_{1m} \\ \mathsf{M} & \mathsf{O} & \mathsf{M} \\ Rss_{1n} & \mathsf{L} & Rss_{nm} \end{pmatrix} \tag{4.4}$$

The distance estimate R is then calculated using:

$$R = \frac{c}{4\pi k F \left(\sqrt[20]{10^{(P_r - P_t - G_r - G_t)}} \right)} \tag{4.5}$$

Effectiveness of this new ranging technique has been measured by comparing the RMSE values for the combined diverse channel and the single channel.

$$RMSE_{(1,m)} = \sqrt{\frac{\sum (P_{r(1,m)} - \mu)^2}{m}} \tag{4.6}$$

Where $$\mu = \frac{\sum (P_{r(1,1)} + P_{r(1,2)} + P_{r(1,3)} + \ldots\ldots P_{r(1,m)})}{m}$$

Eq. (4.6) shows the RMSE of the first channel with m samples. Equation 4.4 shows how the matrix represented by P_r acts as an RSS buffer for all received values for each of the channels. The root mean square error for each channel is then calculated using equation 4.6 where the mean value is calculated for each channel.

4.3. Simulation and Results of the Orthogonal Transmit Model

Table 4.1 shows the recorded distance values in the simulation. Data points from the table were plotted to give rise to Fig. 4.4 which shows the noise and interference that is experienced by each independent channel. An enhanced sample period from the figure has been shown in Fig. 4.5 to make it easier to visualize each channel.

Five data streams have been transmitted through a channel with severe random noise. Each of these channels follow the same general fade path in the form of a gentle exponential decay function. Fig. 4.4 shows the effects of frequency selective fade that is experienced by each band i.e. *920 MHz*, *1187.5 MHz*, *1455 MHz*, *1722.5 MHz* and *1990 MHz*. For a given distance from the transmitter, there are five corresponding data points of RSS values. An aggregation method will be applied to find the best-fit value of RSS [70, 71].

In Fig. 4.5, fifteen delay periods have been used to calculate the distance between transmitter and receiver with the receiver cycling between five ARFCNs. Each of these channels are labeled channel 1 to channel 5.

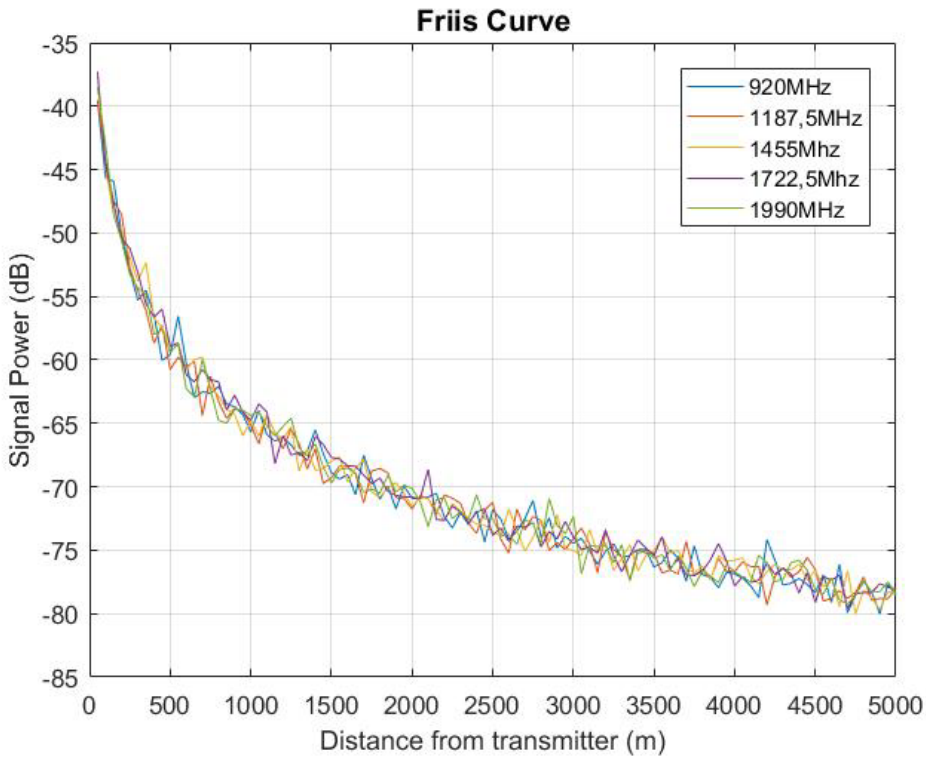

Figure 4.4. Simulation result.

Table 4.1. RSS values for five orthogonal channels with varying levels of SNR

Distance (m)	RSS_1 (dB)	RSS_2 (dB)	RSS_3 (dB)	RSS_4 (dB)	RSS_5 (dB)
50	-39.57681022	-39.51159966	-37.66008882	-37.28571946	-38.51839843
100	-45.64000119	-44.31381864	-44.86699126	-44.58066581	-43.04151833
150	-45.92495102	-47.48319651	-48.55643526	-47.66172578	-48.56445135
200	-50.15011544	-48.55368896	-49.80453397	-50.49504066	-50.63698081
250	-52.98609654	-52.77011145	-51.95304482	-51.20865778	-53.25302114
300	-55.29291797	-54.55415992	-53.77176901	-53.12939983	-54.32148194
350	-54.49553889	-56.10369521	-52.33269089	-55.58823646	-54.87330186
400	-56.41661963	-58.68572757	-56.7270278	-56.63439487	-57.98607039
450	-60.04577223	-57.26039834	-57.44050407	-56.00234787	-57.59084841
500	-59.60021464	-60.75133999	-58.78045981	-58.93640109	-59.4317472
550	-56.55475357	-59.79462003	-58.90836143	-58.66679005	-58.736398
600	-60.29232004	-60.5555858	-60.80555293	-61.15890852	-62.24593597
650	-62.97533493	-60.13065111	-59.96808912	-61.73774189	-62.93132008
700	-62.50750484	-64.39067097	-59.7903873	-60.75670683	-59.99519601
750	-62.6386564	-61.30067909	-62.13346593	-61.57044886	-62.36817406
800	-62.08475012	-63.29858282	-62.8476532	-61.7212362	-64.74759658
850	-63.46865994	-64.59891941	-63.86937265	-63.93909863	-64.99204475
900	-63.70080228	-63.81109701	-64.27595298	-62.7843895	-63.88930061
950	-64.2898593	-64.03864816	-65.97553536	-64.10007516	-63.96461475
1000	-65.67785582	-65.14172443	-64.77124878	-64.76500282	-64.37998312
1050	-63.96850907	-66.61076339	-66.02265878	-63.45216925	-64.07432295
1100	-65.91065512	-64.33896212	-64.289491	-64.10833794	-65.21244092
1150	-66.39489618	-65.73414332	-65.77564399	-68.18256384	-66.00496919
1200	-66.10616408	-67.00802918	-66.24622097	-65.94466452	-65.25339682
1250	-66.7226755	-65.43936173	-65.25717655	-67.50597054	-64.59686611
1300	-67.51792592	-66.62922536	-68.77204416	-67.29594682	-66.96970243
1350	-67.19710434	-68.59171967	-66.99455004	-67.9584527	-67.56472839
1400	-65.52707097	-67.01903938	-68.69799222	-66.01561208	-66.60161426
1450	-67.40360768	-69.74034337	-68.58825794	-66.70381865	-68.45211407
1500	-68.89443919	-69.29719339	-67.98091312	-67.68407337	-69.72243362
1550	-69.39369142	-68.37261821	-67.63246839	-67.82074508	-68.63065061
1600	-69.03882628	-68.38866432	-69.6365508	-68.34176505	-68.55466445
1650	-70.64319494	-68.99670983	-68.51405937	-68.38322363	-68.92141458
1700	-67.50075593	-71.25953376	-67.86809784	-69.07521758	-70.44459258
1750	-69.37402223	-68.75956769	-70.43337189	-69.7567936	-70.17523085
1800	-70.98637463	-68.56122173	-70.81510145	-69.315253	-70.50246699
1850	-69.94035348	-68.89362044	-70.07266272	-70.37086242	-69.10590885

1900	-71.73611913	-70.86293075	-69.66569002	-70.686971	-70.42340129
1950	-69.93587491	-70.91211853	-70.51672174	-70.7879595	-69.86881678
2000	-70.91959411	-71.75556266	-71.55445538	-70.82625882	-70.13961361
2050	-70.91059617	-70.70240008	-70.83745842	-70.94457668	-71.14510651
2100	-70.80007268	-70.90978982	-70.95484596	-68.63011901	-73.14271356
2150	-70.51258331	-72.13777684	-71.81085974	-72.58954099	-71.00335966
2200	-72.37575437	-70.64643689	-72.68647209	-72.63773296	-70.86203275
2250	-73.22822976	-70.90902155	-71.32582113	-71.51512045	-72.51377604
2300	-72.05598169	-71.29495926	-71.93499682	-72.00269693	-71.96900292
2350	-72.96179937	-72.89235032	-72.50187161	-72.8690366	-72.58055016
2400	-71.89677215	-73.66025539	-72.95299104	-71.99476644	-70.62041877
2450	-74.35553479	-71.84862534	-73.0011754	-71.74785951	-72.53141964
2500	-71.81775382	-71.22911223	-73.54352208	-73.83005045	-72.47241115
2550	-72.54193869	-74.13845832	-73.8884255	-73.25619939	-73.89614257
2600	-74.12855744	-75.22518489	-71.75156422	-74.30490212	-73.75236605
2650	-73.49968693	-71.7463381	-73.42390407	-73.09886852	-74.53900881
2700	-72.50694136	-73.40647622	-75.07383543	-73.18100472	-72.61621844
2750	-71.0777173	-72.32637616	-73.99242349	-72.8216079	-72.89699576
2800	-74.0117788	-72.67517594	-72.60030504	-74.74705698	-74.48897474
2850	-72.43246409	-75.03300433	-74.3525799	-73.51693355	-70.92678165
2900	-74.82614415	-74.39736698	-72.18815102	-74.10879695	-73.04635328
2950	-73.90707858	-74.94891035	-74.89348784	-72.72201539	-73.70818001
3000	-74.46745107	-74.08027372	-75.01292575	-73.95320645	-72.34376994
3050	-74.06326848	-73.23722309	-75.43665889	-74.94070972	-76.8592131
3100	-75.04287475	-74.48877667	-73.38092409	-74.77369485	-74.63582602
3150	-76.10513447	-76.78378165	-75.26384587	-75.21996021	-74.70841986
3200	-75.09130245	-73.58523121	-74.40322591	-73.38150703	-74.62059225
3250	-74.51553284	-74.95252443	-76.60332097	-75.46629564	-75.99351062
3300	-75.5939513	-75.54734432	-75.66048299	-76.69464298	-74.5584407
3350	-75.40277311	-77.32160147	-74.55919283	-75.4196679	-77.43554367
3400	-74.94510806	-74.97318539	-76.62750867	-74.20360366	-75.23969069
3450	-74.93468239	-75.22873013	-75.42378658	-74.81061955	-75.03500122
3500	-76.33248284	-75.26031042	-75.05048668	-75.43480525	-75.63988303
3550	-75.99046778	-76.80016096	-73.94364908	-73.93669028	-75.35778662
3600	-74.97298032	-76.57374108	-75.20249157	-76.43129023	-76.60727637
3650	-75.6326255	-76.87971329	-75.01668264	-75.70434971	-75.41386197
3700	-77.42945989	-74.29401004	-76.43581821	-76.95339673	-76.45620083
3750	-74.6502823	-77.01855762	-76.77697126	-76.98607062	-77.85731303
3800	-76.92983741	-76.509912	-76.25672735	-76.65754041	-76.62342927
3850	-77.12531429	-77.31688707	-77.32006602	-75.77912623	-77.04668636
3900	-77.96241596	-75.62807226	-75.416743	-74.48469413	-77.56341206
3950	-76.75910301	-76.6617359	-75.87364188	-75.8505289	-76.14447213
4000	-76.86144067	-76.68591408	-75.79623294	-77.82980602	-76.71825545

4050	-77.1893458	-75.92721289	-75.60584514	-77.07178469	-77.12135943
4100	-77.81279325	-76.29796853	-77.08112438	-77.52764897	-77.52094179
4150	-78.73904167	-76.29252214	-77.65564821	-77.37143377	-75.40189672
4200	-74.17002797	-79.31525523	-76.65688194	-76.00228256	-76.00951166
4250	-75.78446687	-77.0653777	-76.13334764	-76.90791227	-77.47436865
4300	-77.74588947	-76.42061231	-76.52851898	-76.39532349	-77.3003252
4350	-77.6021932	-77.13731976	-76.54173767	-76.88386199	-75.97475377
4400	-77.22768112	-76.68476698	-76.08045183	-78.37946838	-75.79331154
4450	-77.69686631	-75.56354053	-77.38939101	-76.7539109	-76.58210841
4500	-78.35213877	-76.53319234	-76.57768207	-79.13216734	-78.10762646
4550	-76.9437219	-79.00094246	-77.88960247	-77.07796719	-78.46057159
4600	-79.11100216	-78.80277044	-77.18318501	-77.37304795	-77.22109813
4650	-76.1093496	-78.18836653	-79.47017	-76.96615891	-78.93032211
4700	-79.92271536	-78.80207695	-76.61737984	-79.57922772	-79.23036147
4750	-78.57473526	-78.33035089	-80.02630771	-78.45503702	-78.60663772
4800	-77.46976129	-77.11424071	-78.13669694	-78.32444041	-77.38647391
4850	-78.31444811	-78.96372934	-78.77857341	-78.33201207	-78.27308185
4900	-80.02450513	-78.80755513	-79.68043318	-77.64509373	-78.27650853
4950	-77.68779749	-78.83723837	-78.27380638	-77.9089385	-77.48488303
5000	-78.53368391	-78.02240565	-78.36468576	-78.04491305	-78.4623009

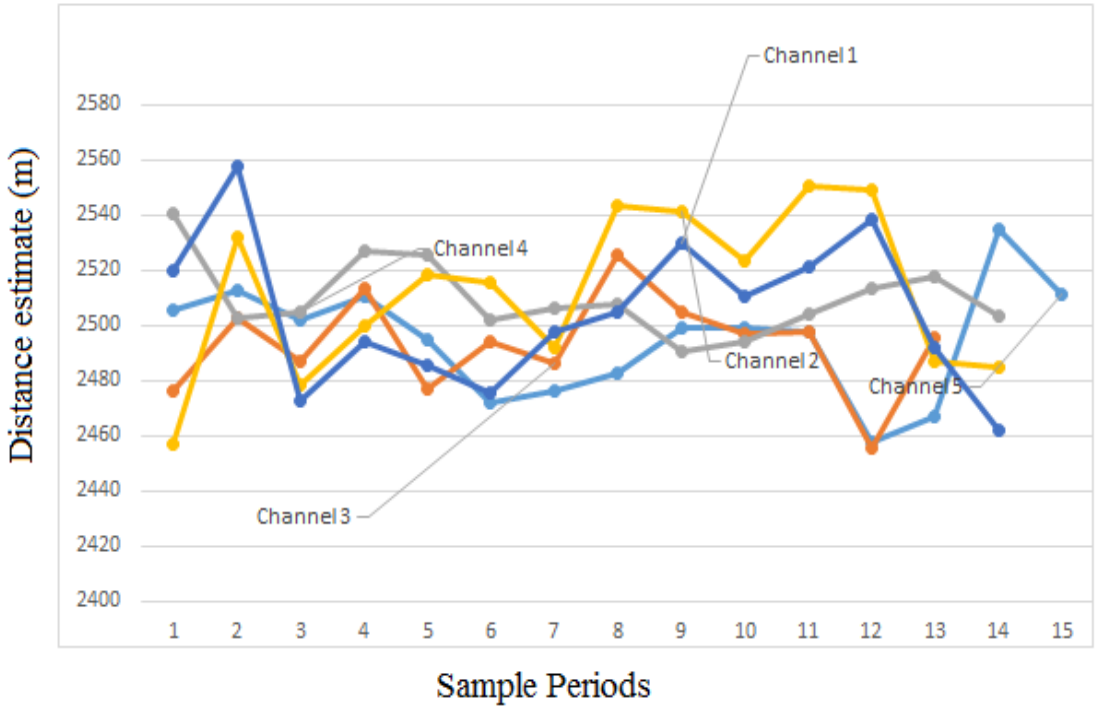

Figure 4.5. Distance estimate values of channels sampled at various periods.

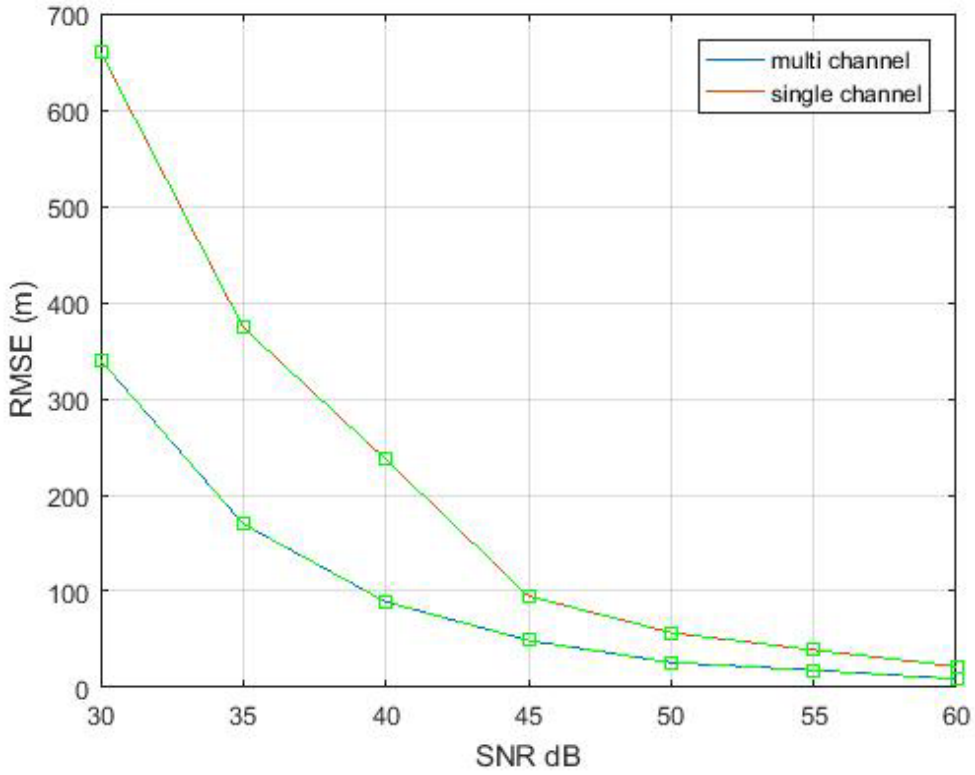

Figure 4.6. RMSE vs SNR for multi-channel and single channel.

- Channel 1 920 MHz
- Channel 2 1187.5 MHz
- Channel 3 1455 MHz
- Channel 4 1722.5 MHz
- Channel 5 1990 MHz

Fig. 4.6 shows the plotted curve of the SNR vs RMSE for the plots in Table 4.1, it can clearly be seen that the RMSE increases more dramatically for a single channel-ranging estimate as compared to that of a multi-channel model.

4.4. Discussion of the Results

The proposed model i.e. Eq. (4.1) is applied over the *920 MHz - 1990 MHz* and split into five distinct channels. To mitigate the effects of RSS shifts due to frequency variation, the constant *k* to provide curve fitting for the five channels. To this effect, each channel should have a similar response regarding distance from the transmitter and the

receiver. The disparity that is shown in Fig. 4.4 is now purely due to noise and interference that is affecting each channel independently.

Data that was recorded in Table 4.1 shows the distance from the transceiver and the RSS value obtained for each of the five channels. When these RSS readings were applied to Eq. 4.5 the distance *R* is found to have a standard deviation of *60 meters* for a typical measured distance. The mean distance was found to be *2497 meters* when each of these channels are simulated under extreme noisy conditions.

Fig. 4.5 shows a close-up of the curve in Fig. 4.4, it clearly demonstrates the effects of noise on the final readings on ranging estimates on each channel. In Fig. 4.6, it can clearly be seen that as the SNR is decreased, RMSE is more pronounced for a single channel range estimation as compared to that of a multi-channel model.

Table 4.2. Test values implemented in Eq. 4.3.

	Value
BTS transmit power	30dB
Gain of the transmitter	5 dB
Gain of the receiver	2 dB
Frequency range	920 MHz-1990 Mhz
Distance	2500 m
Speed of light	$3*10^8$
Signal shadowing	10 dB

4.5. Chapter summary

It has been established that better ranging estimates can be achieved by utilizing frequency diversity techniques compared to conventional models. The results of each channel can then be used in weighting models or even simple aggregation techniques to come up with better accuracy ranging techniques.

Implementation of the above scheme can easily be done using existing network infrastructure since the 3GPP standards have inbuilt diversity schemes imbedded. However further research is required from third party network analysis software

packages like TEMS to break the data frames and isolate each band for analysis to implement the proposed scheme.

CHAPTER 5

Range Improvement by the Use of Quantum Timing on RAN

5.1. Introduction

This chapter intends to improve the accuracy of round trip wave propagation timing on the Um interface to improve ranging estimation. Quantum timing will be used for benchmarking with new timing circuitry that is found natively on the RAN network. Quantum clocks have been in use for a long time for keeping very accurate time with negligible clock drift. GPS utilises quantum clocks to triangulate and find the position of mobile devices. Caesium quantum clocks are also used in NTP servers to synchronise mobile network nodes to mitigate packet loss and frame misalignments.

5.2. Modeling of Quantum Timing of RAN

The proposed method of implementation is illustrated in the block diagram of Fig. 5.1. The serving cell receives a ranging request message on a configured Standalone Dedicated Control Channel (SDCCH) and proceeds by replying with a synchronisation burst on a downlink transceiver (TRX). This synchronisation burst contains a time stamp on one of the Time Division Multiple Access (TDMA) slots. The serving cell uses the time from the NTP server to keep precise time. The MS will receive this time stamp and immediately reply the serving cell on a Fast-Associated Control Channel (FACCH) with a ranging reply. The BTS will calculate the propagation time and therefore the distance of the mobile device from itself.

After the BSC has acquired this information, it transmits this information via the A-interface to the home Mobile Switching Centre (MSC). The MSC will then go through the Visitor Location Register (VLR) and extract location information of the serving cells through Transceiver ID (TRX-ID) or base station Location Area Codes (LAC). This information will be cross-referenced with data in the Home Location Register (HLR) and the exact GPS position of the serving sites will be attained [73].

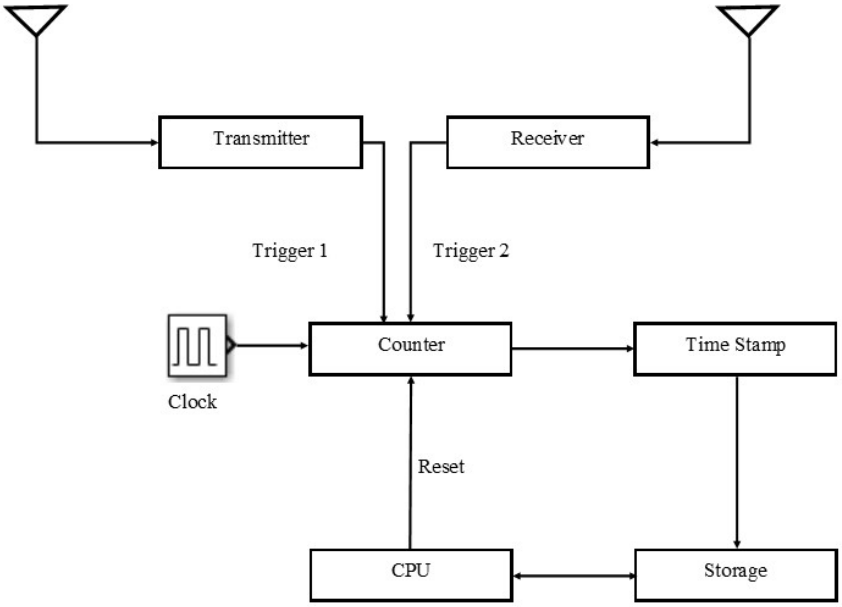

Figure 5.1. Simplified diagram of TDoA circuit at tower.

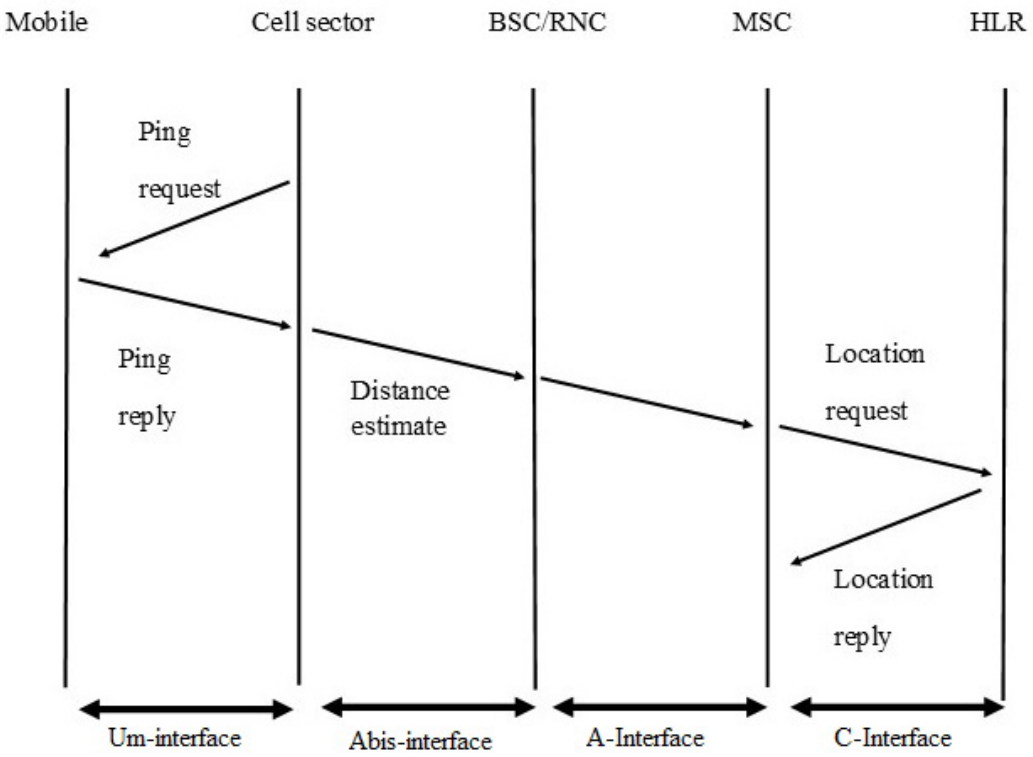

Figure 5.2. Data flow in proposed geo-location setup [16].

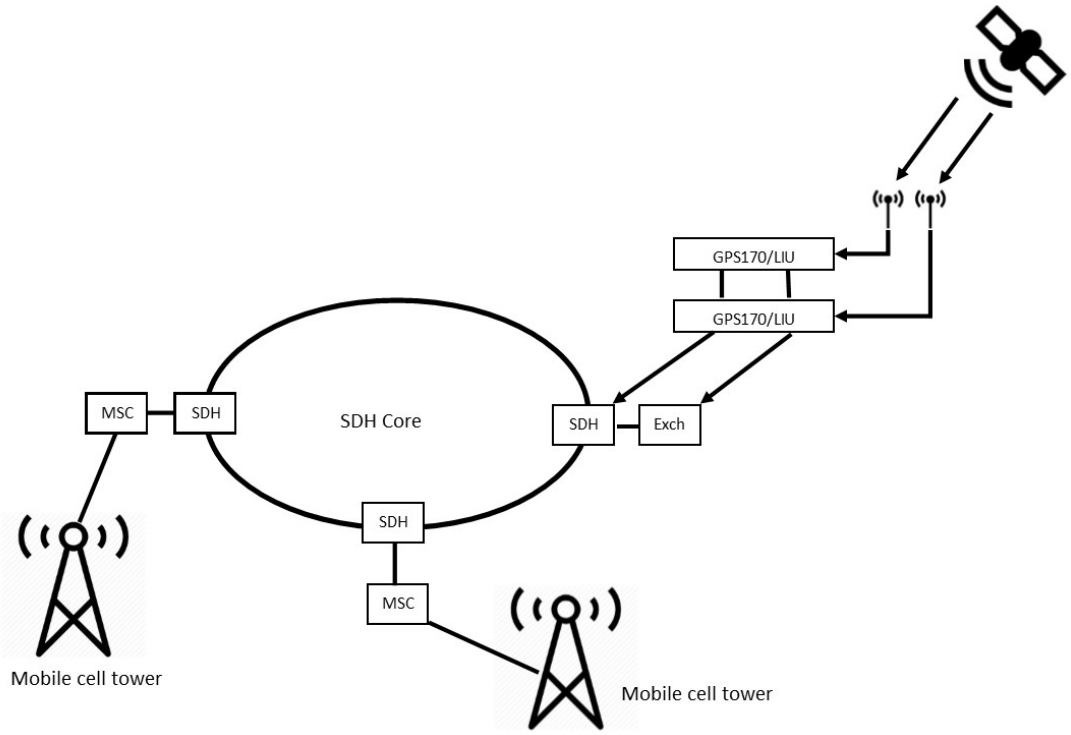

Figure 5.3. Logical representation of timing synchronization with Galileo GPS NTP servers [74].

A minimum of three measurements from three different sites have been used to run a trilateration algorithm to find the exact position of the handset as depicted in Fig. 5.2. Fig. 5.3 shows the synchronisation hierarchy using GPS on SDH transmission. In this setup the satellite clock is used as the absolute time reference in the SDH pool in core-A. Due to the hierarchical nature of SDH, the MSC and subsequent mobile equipment will be synchronised with the caesium clock on the GPS satellite. Then RAN executes the ranging algorithm and calculates the round-trip time for the burst that is sent to the mobile device and back.

5.3. Calculations of Distance Resolution of the Clock

A simulation in MATLAB of *100* orthogonal samples of test distances has been recorded. The calculated distance (D_{cal}) is directly proportional to the resolution of the caesium clock (D_{res}). An algorithm has been developed from Eq. (5.2) and Eq. (5.3) to conclude with a mathematical model of the circuit. Let us assume that the calculated

distance is found by using discrete sampling. As with all wireless technologies, the value of the propagation time (P_{tr}) will not be constant due to various fading properties like multipath and interference. Therefore, the value of (P_{tr}) can be simulated by the diagram and the propagation time can be calculated using:

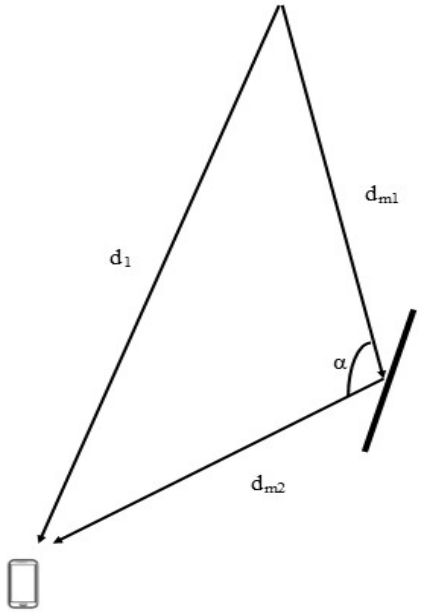

$$P_{(t,r)} = \frac{\left(2d_1 + \Delta d\right)}{c} \tag{5.1}$$

where c is the speed of light, Δd is the error in distance measurement due to the path ($d_{m1} + d_{m2}$) and other propagation delay factors. This will cause timing delays that cannot be foreseen. This is highly prevalent in built up areas like cities. Now since we are using discrete sampling, only the integer part of the propagated distance divided by the resolution distance can provide useful ranging information. Hence,

$$D_{cal} = \left(integer\ value\ of \left(\frac{2\Delta d}{D_{res}} \right) \right) . D_{res} \tag{5.2}$$

$$Error = \left| \left(Actual\ Distance \right) - \left(integer\ value\ of \left(\frac{2\Delta d}{D_{res}} \right) \right) . D_{res} \right| \tag{5.3}$$

Simulation is done to give ideal error estimates from samples that are taken from the (RAN) side when measuring the propagation delay and thus calculating the respective distance between the transmitter and receiver. It is assumed that the NTP server is using a clock timed using caesium that oscillates at *9.2 GHz*. The distance resolution of the clock is calculated by division of unity by the frequency of the clock, in this case *9.2 GHz*. Now the system measures one hundred random samples of distance and comes up with resulting data plots of the actual random distance and the error in calculating the sample.

5.4. Analysis of Calculated Distance and Errors

Table 5.1 shows the data points obtained from the quantum timing model. Sample spaces A to E represent five independent tests that were done with five different clocking devices so as to analyse the nature of the output results. Values in the table have been plotted to give rise to curves in Fig. 5.4 and Fig. 5.5. Fig. 5.4 shows the calculated error in each reading data point from the control distance of 3200 meters using a Caesium atomic clock. Fig. 5.6 and Fig. 5.7 show the same ranging estimates and errors but in this case using *25 MHz* quartz clock as the reference clock. Fig. 5.5 shows the calculated distance using frequency diversity in RSS ranging.

The main focus of this section is to determine the error component that is introduced by each clock when measuring different distances. Error magnitudes will be influenced by resolution of each clock. In Fig. 5.4, random distances are measured by the timing mechanism and the time recorded. With each measurement, the estimated distance is calculated from the recorded time multiplied by the speed of electromagnetic wave propagation. The difference in estimated distance and the actual random distance is calculated and plotted in the graph. In Fig. 5.5, the actual distance that is generated by the random number generator is plotted. This distance has a mean of *3200 meters* and a variance of a few meters.

Table 5.1. (a) Calculated distance

Distance calculated (m)				
Sample space A	**Sample space B**	**Sample space C**	**Sample space D**	**Sample space E**
3235.344	3238.236	3209.268	3244.944	3251.484
3232.896	3221.94	3216.336	3253.632	3240.576
3252.324	3259.812	3206.112	3215.304	3231.888
3216.612	3214.224	3226.332	3208.644	3218.628
3219.756	3239.484	3216.168	3214.272	3242.532
3208.032	3236.688	3218.544	3221.64	3223.512
3256.44	3223.836	3226.056	3217.932	3234.492
3239.076	3209.388	3208.032	3255.72	3253.38
3229.284	3202.476	3230.208	3204.024	3250.728
3238.716	3225.84	3242.676	3235.956	3254.028
3233.136	3211.86	3215.364	3210.6	3256.392
3239.184	3243.816	3247.308	3250.464	3249.108
3233.088	3222.84	3205.368	3210.876	3201.072
3243.54	3250.644	3224.232	3230.628	3201.18
3231.816	3244.308	3201.192	3259.956	3206.16
3259.62	3234.684	3214.008	3221.964	3216.372
3213.9	3211.428	3201.072	3203.772	3202.344
3207.24	3257.484	3212.16	3213.6	3226.02
3207.468	3216.648	3209.4	3224.472	3221.112
3204.744	3255.54	3216.816	3220.68	3232.932
3224.868	3214.2	3211.308	3214.536	3255.636
3227.448	3223.032	3209.172	3256.224	3218.604
3222.576	3206.16	3236.328	3241.308	3220.944
3246.036	3238.764	3254.16	3257.76	3251.7
3238.044	3211.656	3256.416	3226.836	3221.088
3246.54	3203.652	3214.044	3256.476	3209.148
3256.032	3243.66	3229.476	3201.336	3230.952
3258.384	3221.496	3223.176	3237	3251.532
3212.328	3239.976	3231.9	3248.256	3223.668
3209.184	3223.644	3216.624	3214.74	3242.04
3242.076	3238.008	3205.032	3256.008	3238.044
3206.532	3202.272	3226.74	3246.024	3227.568
3231.996	3254.712	3211.248	3249.756	3228.936
3232.284	3248.232	3202.536	3234.828	3257.028
3251.796	3245.004	3257.316	3247.752	3205.92
3229.596	3248.964	3226.404	3220.404	3217.5
3224.208	3223.608	3257.724	3214.176	3227.364
3240.612	3237.408	3245.976	3219.42	3235.656

3244.728	3234.948	3201.432	3235.476	3252.78
3231.672	3232.272	3241.116	3249.96	3228.672
3221.508	3217.224	3242.64	3218.136	3226.8
3209.844	3215.664	3239.052	3224.748	3245.016
3235.572	3227.64	3233.58	3251.856	3228.6
3216.456	3214.428	3213.864	3237.264	3251.784
3203.616	3248.46	3246.564	3259.476	3228.516
3245.532	3259.176	3214.452	3213.012	3230.388
3215.316	3202.764	3222.876	3249.804	3229.752
3227.1	3232.596	3253.56	3240.864	3214.536
3241.572	3206.136	3251.52	3215.688	3206.04
3222.192	3248.316	3224.736	3229.068	3204.972

Table 5.1. (b) Error in measurement.

Errors (m)				
Sample space A	**Sample space B**	**Sample space C**	**Sample space D**	**Sample space E**
0.008700707	0.004135322	0.007066197	0.003203518	0.00654159
0.00762089	0.009345461	0.011681453	0.011764106	0.00102943
0.002520909	0.011193025	0.010090951	0.009599791	0.003930638
0.009962562	0.00211844	0.002442888	0.002221574	0.002109196
0.010370453	0.010613305	0.011684301	0.007005046	0.00217564
0.001657922	0.006447873	0.011767665	0.010821221	0.003041683
0.00993875	0.011480458	0.010646291	0.005992176	0.00141487
0.011560623	0.001042398	0.001228306	0.001792424	0.003796363
0.004330272	0.006964157	0.000948504	0.003511652	0.006008051
0.003700701	0.005622972	0.002026425	0.011338557	0.001114794
0.002250521	0.001917076	0.006828988	0.011035113	0.009182395
0.007377337	0.004740781	0.011134834	0.001940411	0.0026742
0.001270106	0.011398504	0.003285035	0.010094882	0.008111898
0.001750614	0.008045161	0.007122192	0.001836309	0.002351156
0.011223041	0.01155178	0.008253255	0.004439263	0.000660163
0.008572823	0.006526497	0.011936624	0.005021925	0.010913721
0.001921312	0.0064484	0.004733553	0.005584863	0.001121568
0.002098122	0.001657333	0.001600589	0.005974522	0.00100431
0.004150407	0.006000135	0.006559234	0.000508322	0.010833166
0.007890888	0.010272819	0.000483948	0.006422642	0.007882065
0.002219756	0.002453877	0.010631855	0.010549386	0.007975872
0.006001812	0.008264651	0.008289324	0.007090473	0.007467376
0.007154433	0.002520625	0.006251012	0.000138297	0.003002837

0.01077381	0.002876347	0.002416435	0.004713948	0.009326325
0.001886397	0.000396377	0.007406187	0.00441748	0.000220335
0.006842748	0.006015341	0.0058829	0.003862611	0.00110378
0.006360646	0.007235272	0.001611148	0.00822515	0.008138366
0.007710386	0.002821089	0.00865584	0.008114774	0.010732137
0.001672616	0.000392646	0.003022181	0.007469661	0.006503455
0.009577967	0.004247463	0.003483019	0.005910471	0.005764683
0.003713888	0.005443644	0.001076008	0.007651879	0.00234649
0.00338158	0.005339063	0.003297571	0.008503745	0.004901107
0.002859828	0.011629323	0.009329205	0.004522842	0.007458584
0.006308885	0.00096072	0.004319381	0.006351728	0.004674857
0.011248872	0.001001576	0.010018171	0.010318183	0.006356146
0.01034668	0.009656003	0.001194672	0.009430555	0.00990628
0.005925312	0.007072799	0.007955813	0.008256591	0.009431251
0.002437241	0.011474707	0.006454556	0.010794179	0.010704576
0.006218664	0.006196722	0.001571005	0.010885233	0.000414166
0.011095576	0.001050581	0.006279787	0.00493432	0.004930694
0.007047605	0.005115593	0.011094501	0.001287001	0.007690066
0.005837976	0.00510862	0.01059841	0.002709132	0.008911459
0.007431967	0.006687457	0.006280826	0.005380608	0.006717483
0.010573746	0.007056736	0.004415057	0.005633463	0.004813712
0.006791444	0.002525433	0.005606603	0.004079511	0.008208731
0.009062767	0.004150272	0.001671092	0.006233636	0.00016474
0.008336111	0.005525066	0.005018419	0.001336012	0.006408611
0.001736467	0.008187249	0.004800441	0.011835518	0.00265771
0.007969022	0.001555974	0.006237556	1.87E-05	0.007581712
0.002464414	0.007394993	0.007579439	0.003351968	0.003615503

Random distances has been generated in Fig. 5.6, that have a mean of *3200 meters* and a variance of a few meters. Like with the first case above, the estimated distance has been calculated from the recorded time multiplied by the speed of electromagnetic wave propagation. The difference in estimated distance and the actual random distance is calculated and plotted in the graph. The actual distance that is generated by the random number generator has been plotted in Fig. 5.7.

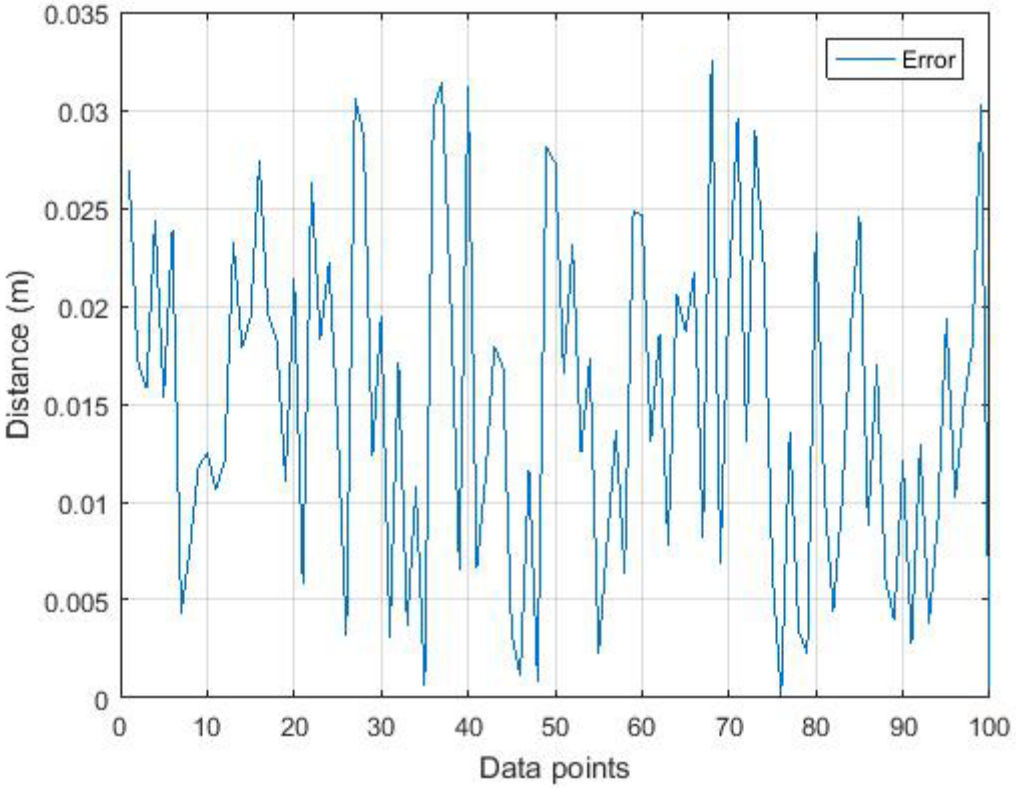

Figure 5.4. Error in range estimate (*Caesium*).

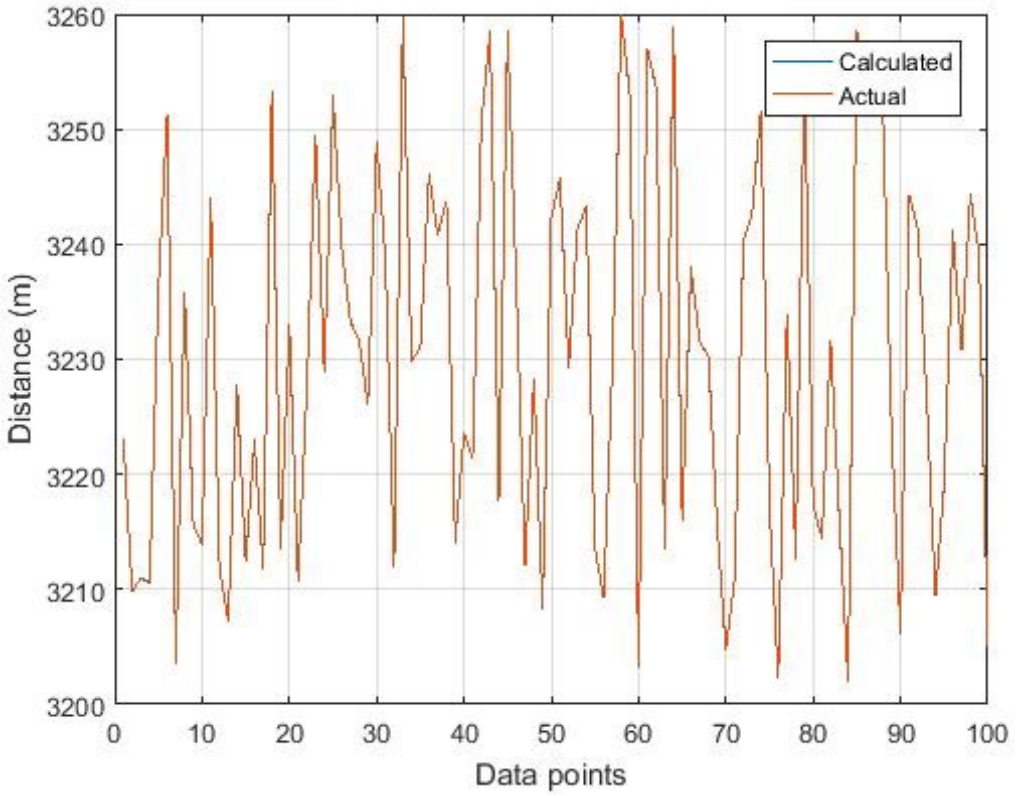

Figure 5.5. Calculated range and error in range calculation (*Caesium*).

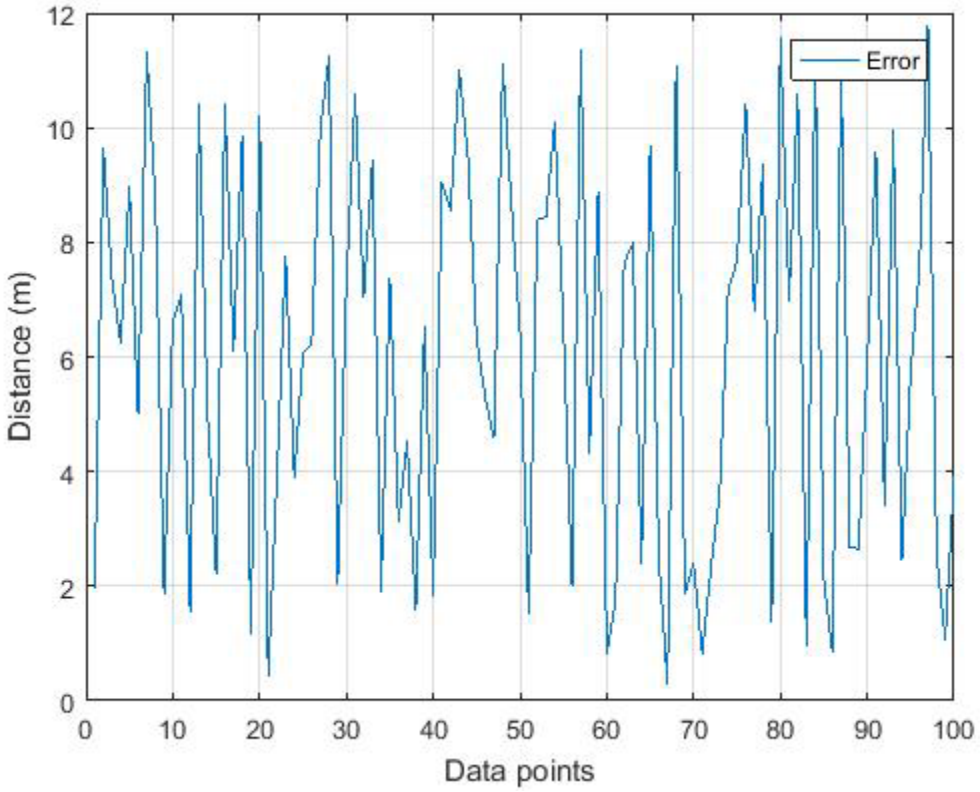

Figure 5.6. Error in range estimate (*25 MHz Quartz).*

5.5. Analysis of Quantum Clock Resolution

This simulation shows the behaviour of quantum timing with varying distances between receiver and transmitter, due to the varying resolution of each clock. It has been deduced that the highest resolution clock with a closer margin of error is the quantum caesium clock. The quartz clock shows deviation from the true value in the values of tens of meters. However, if multipath and the time needed by the system to handle DSP algorithms this value will increase exponentially.

This simulation has without doubt shown that quantum clocks have better resolution when it comes to precise time keeping compared to the quartz oscillators. Table 5.1 is shows the distance estimate extrapolated from the round-trip times for a signal sent from a mobile device and back to the transmitter. A table for the error in calculation and the actual distance measured is shown. The data points in the table are plotted in Fig. 5.4 and Fig. 5.5 for a better visualization of the trend. The measured distance deviates slightly from the actual distance of *3200 meters*.

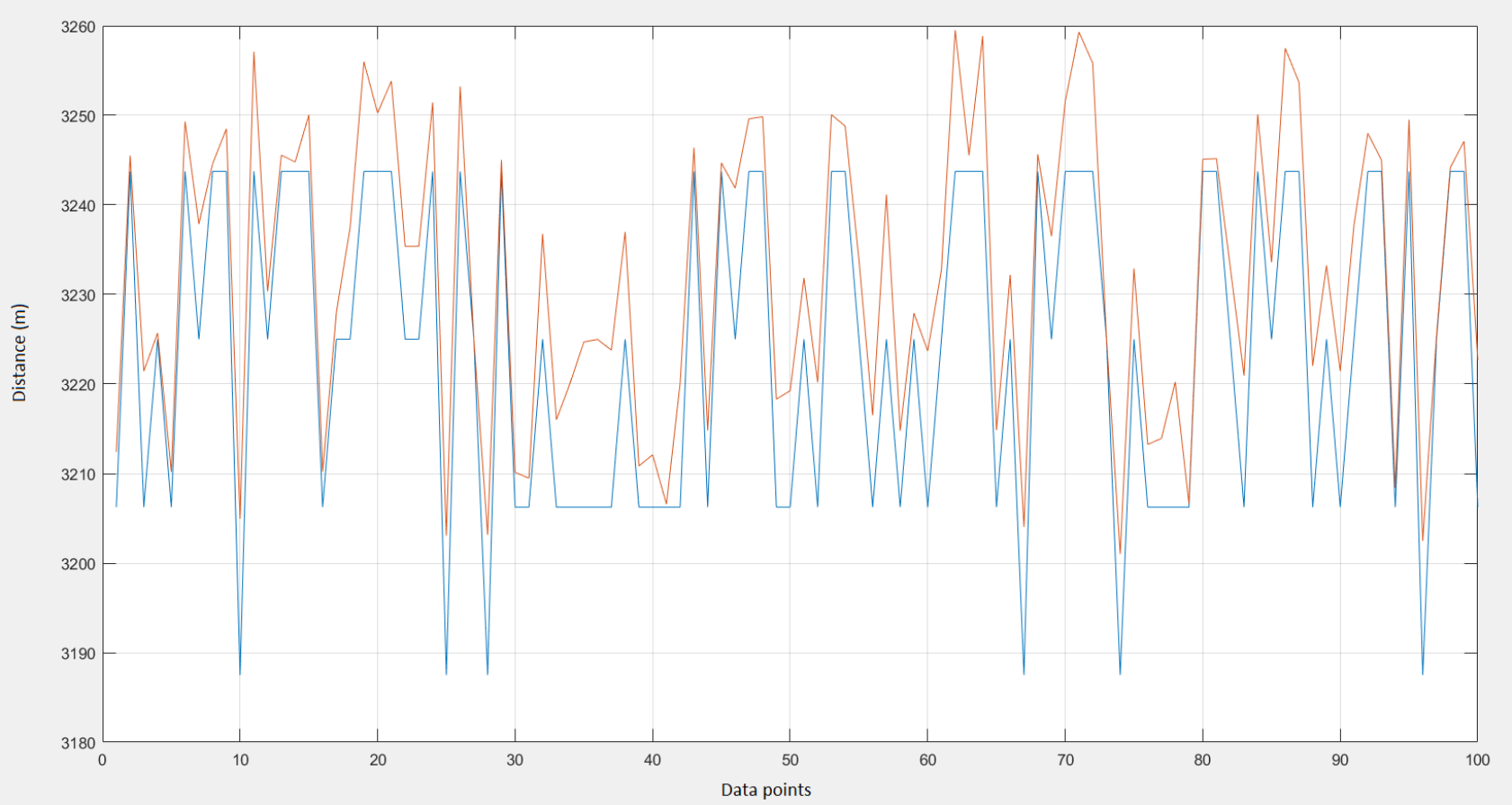

Figure 5.7. Actual distance superimposed with error in calculation (*25 MHz Quartz*).

Based on calculated results from the above table, range approximation errors are highly insignificant. This however doesn't portray the actual behaviour in real world conditions due to transmission bottlenecks and lag introduced by the various network elements during digital signal processing. However, these results are very promising and show that more research is needed to enhance timing circuitry in LBS. Higher the operating frequency of the oscillator, results the greater ranging resolution.

5.6. Chapter Summary

Quantum timing is a viable alternative to traditional TDoA methods that rely on the baseband processing unit of the cell tower for ranging algorithms as shown by its primary use in GPS satellites earlier discussed in the literature review where superior clocking mechanisms are primary in trilateration.

The major drawback for the implementation of quantum timing is the capital expenditure required to integrate a dedicated NTP server for ranging applications. However, small portable quantum time pieces are being developed and deployed that cost a lot less that the models that are sent up on satellites. This could open a whole new dimension in everyday use of extremely precise portable timing devices.

CHAPTER 6

Conclusions and Future Aspects

6.1. Conclusions for RSS Model

This model developed a method of distance approximation by factoring in a constant of proportionality k that varied with each downlink frequency band. We have shown that consideration of frequency provides better geo-location accuracy and tries to address the issue of mitigating distance estimation variances with frequency shifts. This theory backs up the hypothesis that no one universal formula is suitable for distance estimation using RSS values.

Future research in this area includes a hybrid of this technique with other geo-location methods and incorporating this formula in localization algorithms that have been proved like the least square localization algorithm for RSS to further enhance approximation

6.2. Conclusions for Diversity Model

Using statistically independent channels for trilateration purposes, enhances the effective accuracy of range measurement has been observed by the results. Error estimates for the multi-channel calculation offer better SNR vs RMSE curves compared to a single channel. Further development could be the design of an android application (APK) package on an android that can utilize this trilateration scheme and can run multiple scenarios and prove this technique.

6.3. Conclusions for Enhanced Timing Model

Based on results obtained in the previous section, with high precision clocks, it is possible to minimize range estimate errors to an order of *0.035 meters*. This is essentially in the tolerance ranges of GPS accuracy. In this research work, a better passive cell tower location can be achieved by enhancing the current existing methods by either using hybrid techniques that consider the Timing Advance (TA) techniques, received signal strength, angle of arrival or using new unique means like better timing clocks etc.

In future, detailed field tests can be performed to verify the actual delays and errors that have been proposed in this new work. Cell tower geo-location can reach precision that rivals that of GPS of lying within a few meters. Advanced timing mechanisms of GPS have for the first time been extended to cell tower geo-location.

6.4. Comparison of Past Research and This Work

Below is published mean errors and precision for various geo-location techniques by *Andreas Schmidt-Dannert* [5]. Quantum timing has the possibility to reduce ranging estimates to the order of 0.035m which would prove to offer better resolution than current GPS and Assisted GPS, RSS based ranging has the possibility to reduce ranging errors to the order of *60 m* which is in line with current EOTDoA, OTDoA and pilot correlation method.

Table 6.1. Accuracy and precision for various ranging methods

References	Approach	Accuracy
[30]	Cell ID	526 m
[31]	Cell ID+TA	80 m-800 m
[12]	Angle of Arrival	100 m-200 m
[30]	Time Difference of Arrival	624 m
[12]	Uplink TDoA	<50 m
[8]	Pilot Correlation Method	80 m
[8]	Database Correlation Method	25 m
[8]	Observed TDoA	97 m
[31]	Enhanced Observed TD	80 m-110 m
[12]	GPS	5 m-30 m
[31]	Assisted GPS	15 m-100 m
This work	Frequency diversity	60 m
This work	RSS based with specific band	124 m
This work	Quantum timing	0.035 m

6.5. Future Recommendations

Further work should be done to merge these methods of improving accuracy with already established methods like weighted centroid algorithms. Other ways of improving the current designs would be to combine two or more ranging techniques that have been explained in this thesis with other techniques to come up with a hybrid technique of triangulation that would calculate relative parabolas and then find a line of best fit for the position of a device.

For network dependent triangulation applications, to minimize the effects of signaling and digital signal processing between the mobile device and a service control point like the HLR and MSC, a dedicated server that handles location based services can be implemented.

This would be a good idea in implementation of network based services, it should be understood that 3GPP has developed standards for certain interfaces for the GSM and WCDMA protocol stack. Therefore, the only practical approach to implement these rafts of measures would be to develop a mobile application that would communicate with a central location-based server on a predefined internet protocol (IP) address.

Appendix A

```
**************************************************************************
Code for comparing Quantum timing with Quartz oscillator
**************************************************************************

Frequency = [16e6,25e6,30e6,1420405751.7667,6834682610.904324,9192631770];
%Frequencies of test oscillators
c = 3e8;%Speed of propagation wave
Resolution = zeros(1,6);% 1x6 matrix with default null values
ResolutionD = zeros(1,6);% 1x6 matrix with default null values
for g = 1:6
  Resolution(g) = 1/Frequency(g);%Calculation of resolution time space
  ResolutionD(g) = Resolution(g)*c;% Calculation of resolution distance
end
DistanceActual = 3200; %Actual distance between transmitter and receiver
xmin=1;
xmax=60;
n=100; %number of samples
x=xmin+rand(1,n)*(xmax-xmin); %random variable with variance between 1 and 60
meters
Distance = zeros(1,100);% 1x100 matrix with default null values
D = zeros(1,100);% 1x100 matrix with default null values
D1 = zeros(1,100);% 1x100 matrix with default null values
divisor = zeros(1,100);% 1x100 matrix with default null values
buffer1 = zeros(1,100);% 1x100 matrix with default null values
y = 1:100;

for i = 1:100 % loop for 100 data points
    Distance(i) = (DistanceActual + x(i));% equivalent distance
    r = rem(Distance(i),ResolutionD(1)); % check for integer values
```

```
    if(r==0)
      D1(i)=  D(i);%if integer, then save in matrix
    else
       divisor(i) = Distance(i)/ResolutionD(1);
       D(i)= fix(divisor(i));% fix to 32 bit integer and hold
       D1(i)= D(i)*ResolutionD(1);%calculated disance by timming circuit
    end
end
plot(y,D1,y,Distance)%plot distance against calculated distance
grid on
hold on
for i = 1:100
    Distance(i) = (DistanceActual + x(i));
    r = rem(Distance(i),ResolutionD(2));
    if(r==0)
      D1(i)=  D(i);
    else
       divisor(i) = Distance(i)/ResolutionD(2);
       D(i)= fix(divisor(i));
       D1(i)= D(i)*ResolutionD(2);
    end
end
plot(y,D1,y,Distance)
grid on
hold on
```

Appendix B

```
**************************************************************************
Code for plotting RSS power against distance
**************************************************************************
%Variable declaration
Pt = 30; %BTS transmit power
Gt = 5;  %Gain of the transmitter
Gr = 2;  %Gain of the receiver
f = linspace(920e6,1990e6,5); %Division of downlink frequency
c = 3*10^8; %speed of light
R = linspace(50,5000,100); %Distance from sight\
Pr1 = zeros(1,100);
Pr2 = zeros(1,100);
Pr3 = zeros(1,100);
Pr4 = zeros(1,100);
Pr5 = zeros(1,100);

for i = 1:100
    Pr1(i) = Pt+Gt+Gr+(20*log10(c/(4*pi*f(1)*R(i)))) ;
end
for i = 1:100
    Pr2(i) = Pt+Gt+Gr+(20*log10(c/(4*pi*f(2)*R(i)))) ;
end
for i = 1:100
    Pr3(i) = Pt+Gt+Gr+(20*log10(c/(4*pi*f(3)*R(i)))) ;
end
for i = 1:100
    Pr4(i) = Pt+Gt+Gr+(20*log10(c/(4*pi*f(4)*R(i)))) ;
end
```

```
for i = 1:100
    Pr5(i) = Pt+Gt+Gr+(20*log10(c/(4*pi*f(5)*R(i)))) ;
end
plot(R,Pr1,R,Pr2,R,Pr3,R,Pr4,R,Pr5);
grid on
legend('920MHz','1187,5MHz','1455Mhz','1722,5Mhz','1990MHz')
xlabel('Distance from transmitter (m)')
ylabel('Signal Power (dB)')
title('Friis Curve','FontSize',12)
```

****

Code for curve fitting RSS value with varying Frequency to find constant k

****

```
%Variable declaration
Pt = 30; %BTS transmit power
Gt = 5;  %Gain of the transmitter
Gr = 2;  %Gain of the receiver
f = linspace(920e6,1990e6,5); %Division of downlink frequency
c = 3*10^8; %speed of light
R = linspace(50,5000,100); %Distance from sight\
Pr1 = zeros(1,100);
Pr2 = zeros(1,100);
Pr3 = zeros(1,100);
Pr4 = zeros(1,100);
Pr5 = zeros(1,100);

for i = 1:100
    Pr1(i) = Pt+Gt+Gr+(20*log10(c/(4*pi*f(1)*R(i)))) ;
end
for i = 1:100
    Pr2(i) = Pt+Gt+Gr+(20*log10(c/(4*pi*f(2)*R(i)*0.7747))) ;
end
```

```
for i = 1:100
    Pr3(i) = Pt+Gt+Gr+(20*log10(c/(4*pi*f(3)*R(i)*0.6323))) ;
end
for i = 1:100
    Pr4(i) = Pt+Gt+Gr+(20*log10(c/(4*pi*f(4)*R(i)*0.5341))) ;
end
for i = 1:100
    Pr5(i) = Pt+Gt+Gr+(20*log10(c/(4*pi*f(5)*R(i)*0.4623))) ;
end
plot(R,Pr1,R,Pr2,R,Pr3,R,Pr4,R,Pr5);
grid on
legend('920MHz','1187,5MHz','1455Mhz','1722,5Mhz','1990MHz')
xlabel('Distance from transmitter m')
ylabel('Signal Power dB')
title('Friis Curve','FontSize',12)
```

****

Code for plotting bar graph for RSS values vs calculated estimated distance

****

```
%Variable declaration
Pr = -50;
Pt = 30;
Gt = 5;
Gr = 2;
c = 3*10^8;
f = linspace(920e6,1990e6,5);

PR = zeros(1,5);
R1 = (c)/((nthroot((10^(Pr-Pt-Gt-Gr)),20))*4*f(1)*pi);
R2 = (c)/((nthroot((10^(Pr-Pt-Gt-Gr)),20))*4*f(2)*pi);
R3 = (c)/((nthroot((10^(Pr-Pt-Gt-Gr)),20))*4*f(3)*pi);
R4 = (c)/((nthroot((10^(Pr-Pt-Gt-Gr)),20))*4*f(4)*pi);
```

```
R5 = (c)/((nthroot((10^(Pr-Pt-Gt-Gr)),20))*4*f(5)*pi);
PR(1) = R1;
PR(2) = R2;
PR(3) = R3;
PR(4) = R4;
PR(5) = R5;
B = std2(PR)
bar(f,PR)
grid on
xlabel('Frequency(Hz)')
ylabel('Distance from transmitter (m)')
title('Distance estimation with RSS value of -50dB','FontSize',12)

**************************************************************************
Code for standard deviation in input buffer for calculated distances
**************************************************************************

Frequency = linspace(5e6,9192631770,100); %Hz
c = 3e8;
Resolution = zeros(1,100);% 1x6 matrix with default null values
ResolutionD = zeros(1,100);% 1x6 matrix with default null values
for g = 1:100
  Resolution(g) = 1/Frequency(g);%Calculation of resolution time space
  ResolutionD(g) = Resolution(g)*c;% Calculation of resolution distance
end
DistanceActual = 3200;
xmin=1;
xmax=60;
n=100;
x=xmin+rand(1,n)*(xmax-xmin);
Distance = zeros(1,100);
D = zeros(1,100);
D1 = zeros(1,100);
```

```
divisor = zeros(1,100);
buffer1 = zeros(1,100);
y = 1:1000;

for i = 1:100
      Distance(i) = (DistanceActual + x(i));
      divisor(i) = Distance(i)/ResolutionD(i);
      D(i)= fix(divisor(i));
      D1(i)= D(i)*ResolutionD(i);
end
  for t = 1:100
   buffer1(t)= (Distance(t)-D1(t));
end
RMSE = sqrt(mean((buffer1).^2));
plot (buffer1)
```

Appendix C

```
**************************************************************************
Code for diversity
**************************************************************************

%Variable declaration
Pt = 30; %BTS transmit power
Gt = 5;  %Gain of the transmitter
Gr = 2;  %Gain of the receiver
f = linspace(920e6,1990e6,5); %Division of downlink frequency
c = 3*10^8; %speed of light
R = linspace(50,5000,100); %Distance from sight\
Pr1 = zeros(1,100);
Pr2 = zeros(1,100);
Pr3 = zeros(1,100);
Pr4 = zeros(1,100);
Pr5 = zeros(1,100);

for i = 1:100
    n =randn;
    Pr1(i) = ((Pt+Gt+Gr+(20*log10(c/(4*pi*f(1)*R(i)))))+n)-10;
end
for i = 1:100
    n =randn;
    Pr2(i) = ((Pt+Gt+Gr+(20*log10(c/(4*pi*f(1)*R(i)))))+n)-10 ;
end
for i = 1:100
    n =randn;
    Pr3(i) = ((Pt+Gt+Gr+(20*log10(c/(4*pi*f(1)*R(i)))))+n)-10 ;
```

```
end
for i = 1:100
    n =randn;
    Pr4(i) = ((Pt+Gt+Gr+(20*log10(c/(4*pi*f(1)*R(i)))))+n)-10 ;
end
for i = 1:100
    n =randn;
    Pr5(i) = ((Pt+Gt+Gr+(20*log10(c/(4*pi*f(1)*R(i)))))+n)-10 ;
end
plot(R,Pr1,R,Pr2,R,Pr3,R,Pr4,R,Pr5);
grid on
legend('920MHz','1187,5MHz','1455Mhz','1722,5Mhz','1990MHz')
xlabel('Distance from transmitter (m)')
ylabel('Signal Power (dB)')
title('Friis Curve','FontSize',12)

Power1 = zeros(1,1000);
Power2 = zeros(1,1000);
Power3 = zeros(1,1000);
Power4 = zeros(1,1000);
Power5 = zeros(1,1000);

for i = 1:1000
n =randn;
Power1(i) = ((Pt+Gt+Gr+(20*log10(c/(4*pi*f(1)*2500))))+n)-10;
n =randn;
Power2(i) = ((Pt+Gt+Gr+(20*log10(c/(4*pi*f(2)*2500))))+n)-10;
n =randn;
Power3(i) = ((Pt+Gt+Gr+(20*log10(c/(4*pi*f(3)*2500))))+n)-10;
n =randn;
Power4(i) = ((Pt+Gt+Gr+(20*log10(c/(4*pi*f(4)*2500))))+n)-10;
n =randn;
```

```
Power5(i) = ((Pt+Gt+Gr+(20*log10(c/(4*pi*f(5)*2500))))+n)-10;
end

R1 = zeros(1,1000);
R2 = zeros(1,1000);
R3 = zeros(1,1000);
R4 = zeros(1,1000);
R5 = zeros(1,1000);

for i = 1:1000
R1(i) = (c)/((nthroot((10^((Power1(i)+10)-Pt-Gt-Gr)),20))*4*f(1)*pi);
R2(i) = (c)/((nthroot((10^((Power2(i)+10)-Pt-Gt-Gr)),20))*4*f(2)*pi);
R3(i) = (c)/((nthroot((10^((Power3(i)+10)-Pt-Gt-Gr)),20))*4*f(3)*pi);
R4(i) = (c)/((nthroot((10^((Power4(i)+10)-Pt-Gt-Gr)),20))*4*f(4)*pi);
R5(i) = (c)/((nthroot((10^((Power5(i)+10)-Pt-Gt-Gr)),20))*4*f(5)*pi);
End
```

References

[1] K. Sriram P. Varshney, and J. Shanthikumar, Discrete-time analysis of integrated voice/data multiplexers with and without speech activity detectors," *IEEE Journal on Selected Areas in Communications*, vol. 1, no. 6, pp. 1124-1132, 1983.

[2] Ahmed El Rabbany, *Introduction to GPS: The Global Positioning System*, Artech House, May 2002.

[3] R. B. Langley, "Why is the GPS signal so complex?," *GPS World*, vol. 1, no. 3, pp. 56-59, May/June 1990.

[4] Yunhao Liu and Zheng Yang, *Location, Localization, and Localizability: Location-awareness Technology for Wireless Networks*, Springer, Nov. 2010.

[5] Andreas Schmidt Dannert, "Positioning technologies and mechanisms for mobile devices," *Seminar Master Module SNET2*, TU-Berlin.

[6] Jie Yang, Alexander Varshavsky, Hongbo Liu, Yingying Chen, and Marco Gruteser, "Accuracy characterization of cell tower localization,"*12th International Conference on Ubiquitous Computing (UbiComp 2010)*, Copenhagen, Denmark, 26-29 Sept. 2010, pp. 223-226.

[7] Yan Cui, Ruxiao An, and Kartik B. Ariyur, "Cellphone geolocation via magnetic mapping," *Automatica*, vol. 51, pp. 70-79, Jan. 2015.

[8] Rinku Dewri and Ramakrishna Thurimella, "Mobile local search with noisy locations," *Pervasive and Mobile Computing*, vol. 32, pp. 78-92, Oct. 2016.

[9] Robson D. A. Timoteo, Lizandro N. Silva, Daniel C. Cunha, and George D. C. Cavalcanti, "An approach using support vector regression for mobile location in cellular networks," *Computer Networks*, vol. 95, pp. 51-61, Feb. 2016.

[10] Jie Yang, Alexander Varshavsky, Hongbo Liu, Yingying Chen, and Marco Gruteser, "Accuracy characterization of cell tower localization," *12th International Conference on Ubiquitous Computing*, 26-29 Sept. 2010, pp. 223-226.

[11] Robert P. Biuk Aghai, “GSM-based provider-independent positioning method,” *Location Asia 2007*, Hong Kong, China, 13-14 Sept. 2007, pp. 1-9.

[12] Postal and Telecommunication Regulatory Authority of Zimbabwe (POTRAZ) 2017, “*Abridged postal & telecommunications sector performance report: first quarter 2017*,” www.potraz.gov.zw/images/documents/Abridged_Sector_ Perfomance_ report_1st_Quarter_2017.pdf, accessed 19 October 19, 2017,

[13] Petre Stoica and Jian Li, “Source localization from range-difference measurements,*” IEEE Signal Processing Magazine*, vol. 23, no. 6, pp. 63-69, Nov. 2006.

[14] Julius O. Smith and Jonathan S. Abel, “Closed-form least-squares source location estimation from range-difference measurements,” *IEEE Trans. on Acoustics, Speech and Signal Processing*, vol. 35, no. 12, pp. 1661-1669, Dec. 1987.

[15] Thavisak Manodham, Luis Loyola, and Tetsuya Miki, “A novel wireless positioning system for seamless internet connectivity based on the WLAN infrastructure,” *Wireless Personal Communications*, vol. 44, no. 3, pp. 295–309, Feb. 2008.

[16] Nikos Deligiannis and Spiros Louvros, “Hybrid TOA–AOA location positioning techniques in GSM networks,” *Wireless Personal Communications*, vol. 54, no. 2, pp. 321–348, July 2010.

[17] V. K. Jain, Shashikala Tapaswi, and Anupam Shukla, “Performance analysis of received signal strength fingerprinting based distributed location estimation system for indoor WLAN,” *Wireless Personal Communications*, vol. 70, no. 1, pp. 113–127, May 2013.

[18] Varun Khaitan, Peerapol Tinnakornsrisuphap, and Mehmet Yavuz, “Indoor positioning using femtocells,” *2011 IEEE Vehicular Technology Conference (VTC Fall)*, San Francisco, CA, USA, 5-8 Sept. 2011, pp. 1-5.

[19] Gabor Fodor, Erik Dahlman, Gunnar Mildh, Stefan Parkvall, Norbert Reider, Gyorgy Miklos, Zoltan Turanyi, “Design aspects of network assisted device-to-device communications,” *IEEE Communications Magazine*, vol. 50, no. 3, pp. 170-177, March 2012.

[20] Holger Karl and Andreas Willig, “Time synchronization,” in *Protocols and Architectures for Wireless Sensor Networks*, John Wiley & Sons, Aug. 2007.

[21] Ciaran McElroy, Dries Neirynck, and Michael McLaughlin, “Comparison of wireless clock synchronization algorithms for indoor location systems,” *IEEE International Conference on Communications Workshops (ICC)*, Sydney, Australia, 10-14 June 2014, pp. 157–162

[22] Hassan A. Karimi, *Advanced location based technologies and services*, CRC Press, April 2016.

[23] R. Tjoa, K. L. Chee, P. K. Sivaprasad, S. V. Rao, and J. G. Lim, “Clock drift reduction for relative time slot TDMA-based sensor networks,” *15th IEEE International Symposium on Personal, Indoor and Mobile Radio Communications*, Barcelona, Spain, 5-8 Sept. 2004, pp. 1042-1047.

[24] Swen Leugner, Mathias Pelka, and Horst Hellbruck, “Comparison of wired and wireless synchronization with clock drift compensation suited for U-TDoA localization,” *13th Workshop on Positioning, Navigation and Communications (WPNC),* Bremen, Germany, 19-20 Oct. 2016.

[25] Ramon M. Cerda, *Understanding Quartz Crystals and Oscillators*, Artech House, 2014.

[26] Vincent R. Von Kaenel, Eric A. Vittoz, and Daniel Aebischer, “Crystal oscillators,” *Chapter in Springer’s Analog Circuit design*, pp. 369-382, 1996.

[27] J. Mendizabal, U. Alvarado, I. Guruceaga, H. Solar, A. Garcia Alonso, and R. Berenguer, “A dual front-end for the new GPS/GALILEO generation in a 0.35μm SiGe process,” *Integration, the VLSI Journal*, vol. 42, no. 3, pp. 321-331, June 2009.

[28] Leo A. Mallette and Joe White, “Space qualified frequency sources (clocks) for current and future GNSS applications,” *IEEE Position Location and Navigation Symposium (PLANS),* 4-6 May 2010, Indian Wells, CA, USA, USA, pp. 903-908.

[29] Ahmed Al Samaneh, *VCSELs for Cesium-Based Miniaturized Atomic Clocks*, Herstellung und Verlag, Books on Demand, Sept. 2015.

[30] Hassan A. Karimi, *Advanced location based technologies and services*, CRC Press, Taylor and Francis Group, April 2016.

[31] F. G. Major, *The Quantum beat: Principles and applications of atomic clocks*, 2nd Ed., Springer-Verlag, New York, USA, June 2007.

[32] Rainer Mautz and Sebastian Tilch, "Survey of optical indoor positioning systems," *International Conference on Indoor Positioning and Indoor Na*vigation (IPIN), Guimaraes, Portugal, 21-23 Sept. 2011, pp. 1-7.

[33] Ann Chen Chang and Jhih Chung Chang, "Robust mobile location estimation using hybrid TOA/AOA measurements in cellular systems," *Wireless Personal Communications*, vol. 65, no. 1, pp. 1–13, Jan. 2011.

[34] Vanshaj Sikri and Tushar Kundra, "GSM enabled wristwatch to send distress message consisting location co-ordinates obtained using cell tower triangulation," *International Conference on Man and Machine Interfacing (MAMI)*, Bhubaneswar, India, 17-19 Dec. 2015, pp. 1-6.

[35] Eneh Joy Nnenna and Orah Harris Onyekachi, "Mobile positioning techniques in GSM cellular networks: A comparative performance analysis," *International Journal of Computer Technology and Electronics Engineering*, vol. 2, no. 6, pp. 21-29, Dec. 2012.

[36] Klaithem Al Nuaimi and Hesham Kamel, "A survey of indoor positioning systems and algorithms," *International Conference on Innovations in Information Technology (IIT)*, Abu Dhabi, UAE, 25-27 April 2011, pp. 185-190.

[37] William C. Y. Lee, *Mobile Communications Design Fundamentals*, 2nd Ed., Wiley Publication, 1993.

[38] Hyeonmu Jeon, Uk Jo, Mingyu Jo, Nammoon Kim, and Youngok Ki, "An adaptive AP selection scheme based on RSS for enhancing positioning accuracy," *Wireless Personal Communications*, vol. 69, no. 4, pp. 1535–1550, April 2013.

[39] J. Salo, L. Vuokko and P. Vainikainen, "Why is Shadow Fading Lognormal?" in Proc. *International Symposium on Wireless Personal Multimedia Communications*, Aalborg, Denmark, Sept. 18-22, 2005, pp. 522-526.

[40] Devendra K. Misra, *Radio-Frequency and Microwave Communication Circuits: Analysis and Design*, 2nd Ed., Wiley Publication, 2004.

[41] Shofiyati N. Karimah, Muhammed R. Kahar, and Tad Matsumoto, "A hybrid TOA and RSS-based factor graph for wireless geolocation technique," *12th Int.*

Colloquium on Signal Processing and Its Applications, Melaka, Malaysia, 4-6 March 2016, pp. 140-145.

[42] Sichun Wang, Robert Inkol, Brad R. Jackson, and Shanzeng Guo, "Ambiguity resolution in RSS-based emitter geolocation," *Int. Conf. on Computing, Networking and Communications*, San Diego, CA, USA, 28-31 Jan. 2013, pp. 508-513.

[43] Zeyuan Li, "Constrained weighted least Squares location algorithm using Received Signal Strength measurements," *China Communications*, vol. 13, no. 4, pp. 81-88, April 2016.

[44] Camillo Gentile, Nayef Alsindi, Ronald Raulefs, and Carole Teolis, *Geolocation Techniques: Principles and Applications*, Springer, New York, USA, Nov. 2012.

[45] Yong S. Cho, Jaekwon Kim, Won Y. Yang, and Chung G. Kang, *MIMO-OFDM Wireless Communications with MATLAB*, 1st Ed., Wiley, Oct. 2010.

[46] Roger L. Freeman, *Radio System Design for Telecommunication*, 3rd Ed., Wiley Interscience-IEEE Press, New York, Nov. 2007.

[47] F. C. Owen and C. D. Pudney, "In-building propagation at 900 MHz and 1650 MHz for digital cordless telephones," *6th Int. Conf. on Antennas and Propagation*, Coventry, UK, 4-7 April 1989, pp. 276-280.

[48] David Tse and Pramod Viswanath, *Fundamentals of Wireless Communication*, Cambridge University Press, May 2005.

[49] V. Umadevi and P. Easwaran, "A study on rake receivers," *International Conference on Electrical, Instrumentation and Communication Engineering (ICEICE 2017)*, Karur, India, 27-28 April 2017, pp. 1-5.

[50] Gregory E. Bottomley, Tony Ottosson and Yi Pin Eric Wang, "A generalized RAKE receiver for interference suppression," *IEEE Journal on Selected Areas in Communications*, vol. 18, no. 8, pp. 1536 – 1545, Aug. 2000.

[51] Anupama Tasneem and Satya Prashad Majumder , "BER performance analysis of a MC-DS-CDMA wireless communication system with rake receiver employing MRC under Nakagami-m fading," *IEEE Transactions on Vehicular Technology, IEEE*, vol. 50, no. 3, pp. 674 – 685, May 2001.

[52] M.A. Spirito, “On the accuracy of cellular mobile station location estimation,” *IEEE Transactions on Vehicular Technology, IEEE*, vol. 50, no. 3, pp. 674-685, May 2001.

[53] Juan Antonio Garcia Fernandez, Antonio Jurado Navas, Mariano Fernandez Navarro, and Carlos Ubeda, “Efficient star-topology solving local minima for geolocation in real UMTS networks: An experimental assessment with real data,” *Wireless Personal Communications*, vol. 85, no. 4, pp. 2115-2140, Dec. 2015.

[54] Adrian N. Bishop, Barıs Fidan, Kutluy Dogancay, Brian D. O. Anderson, and Pubudu N. Pathirana, “Exploiting geometry for improved hybrid AOA/TDOA-based localization,” *Signal processing*, vol. 88, no. 7, pp. 1775-1791, July 2008.

[55] Liu Cheng Chen, Xiao Gong Hu, Chun Hao Han, and Jin Ping Chen, “Research on the fitting algorithms of almanac parameters for navigation satellites,” *Chinese Astronomy and Astrophysics*, vol. 33, no. 1, pp. 90-98, Jan.-March 2009.

[56] Alan Oxley, *Uncertainties in GPS Positioning: A Mathematical Discourse*, Elsevier Academic Press, 2017.

[57] Bernhard Hofmann Wellenhof, Herbert Lichtenegger, and Elmar Wasle, *GNSS – Global Navigation Satellite*, 1st Ed., Springer Wien, New York, USA, 2007.

[58] Peng Dong Ju and Wu Bin, “The effect of GPS ephemeris on the accuracy of precise orbit determination of LEO satellite-borne GPS,” *Chinese Astronomy and Astrophysics*, vol. 33, no. 2, pp. 206-216, April-June 2009.

[59] Heather Graves and Roger Graves, *A Strategic Guide to Technical Communication*, 2nd Ed., Broadview Press, 2012.

[60] Paulo Verissimo and Luis Rodrigues, “Distributed real-time systems and platforms,” *Chapter in Distributed Systems for System Architects*, Springer Advances in Distributed Computing and Middleware, vol. 1, pp. 355-368, 2001.

[61] Dan Doberstein, *Fundamentals of GPS Receivers: A Hardware Approach*, Springer, New York, USA, 2012.

[62] Goran M. Djuknic and Robert E. Richton, *Geolocation and Assisted GPS*, Bell Laboratories, Lucent Technologies, Feb. 2001.

[63] Michel Mouly and Marie Bernadette Pautet, *The GSM system for mobile communications*, Telcom Publishing, 1992.

[64] Xinxin Ouyang, Qun Wan, Jingmin Cao, Jinyu Xiong, and Qing He, “Direct TDOA geolocation of multiple frequency-hopping emitters in flat fading channels,” *IET Signal Processing*, vol. 11, no. 1, pp. 80-85, Feb. 2017.

[65] Jonas Medbo, Iana Siomina, Ari Kangas, and Johan Furuskog, “Propagation channel impact on LTE positioning accuracy: A study based on real measurements of observed time difference of arrival,” *IEEE 20th International Symposium on Personal, Indoor and Mobile Radio Communications*, Tokyo, Japan, 13-16 Sept. 2009, pp. 2213-2217.

[66] Martin Sauter, *From GSM to LTE-Advance: An Introduction to Mobile Networks and Mobile Broadband*, 2nd Ed., Wiley Publication, 2014.

[67] C. Drane, M. Macnaughtan, and C. Scott, “Positioning GSM telephones,” *IEEE Communications Magazine*, vol. 36, no. 4, pp. 46-54, 1998.

[68] Brian Albright, *Essentials of Mathematical Statistics*, 1st Ed., Jones & Bartlett Learning, 2014.

[69] Jorg Eberspacher, Hans Joerg Vogel, Christian Bettstetter, and Christian Hartmann, *GSM - Architecture, Protocols and Services*, John Wiley & Sons, Dec 2008.

[70] Robson T. Reza and Viranjay M. Srivastava, “Effect of GSM frequency band on received signal strength and distance estimation from cell tower,” *10th International Conference on the Developments in e-Systems Engineering (DeSE)*, Paris, France, 14-16 June 2017, pp. 1-4.

[71] Robson T. Reza and Viranjay M. Srivastava, “Improving cell tower geo-location using Quantum clock Timing,” *Int. J. on Communications Antenna and Propagation*, vol. 8, no. x, 2018, accepted.

[72] Robson T. Reza and Viranjay M. Srivastava, “An empirical analysis of a six radio channel pseudo generator for better noise reduction in ranging systems” *Far East J. of Electronics and Communications*, vol. 17, no. 6, pp. 1299-1307, Dec. 2017.

[73] Caimu Tang and Dapeng Oliver Wu, “An Efficient Mobile Authentication Scheme for Wireless Networks,” *IEEE Transactions on Wireless Communications*, vol. 7, no. 4, pp. 1408-1416, April 2008.

[74] Time Synchronization in Telecom Networks, Available at: https://www.meinbergglobal.com/english/info/time-synchronization-telecom-networks.htm, Accessed 17 August 2017.